Journal of Medicinal Chemistry

Article

pubs.acs.org/jmc

Evaluation and Discovery of Novel Synthetic Chalcone Derivatives as Anti-Inflammatory Agents

Jianzhang Wu,[†,‡,§] Jianling Li,[†,§] Yuepiao Cai,[†] Yong Pan,[†] Faqing Ye,[†] Yali Zhang,[‡] Yunjie Zhao,[†] Shulin Yang,[‡] Xiaokun Li,[†] and Guang Liang*[,†,‡]

[†]School of Pharmacy, Wenzhou Medical College, 1210 University Town, Wenzhou, Zhejiang 325035, China

[‡]College of Chemical Engineering, Nanjing University of Science and Technology, 200 Xiaolingwei Street, Nanjing, Jiangsu 210094, China

Supporting Information

ABSTRACT: Major anti-inflammatory agents, steroids and cyclooxygenase, were proved to have serious side effects. Here, a series of chalcone derivatives were synthesized and screened for anti-inflammatory activities. QSAR study revealed that the presence of electron-withdrawing groups in B-ring and electron-donating groups in A-ring of chalcones was important for inhibition of LPS-induced IL-6 expression. Further, compounds **22**, **23**, **26**, **40**, and **47** inhibited TNF-α and IL-6 release in a dose-dependent manner and decreased LPS-induced TNF-α, IL-1β, IL-6, IL-12, and COX-2 mRNA production. Mechanistically, compounds **23** and **26** interfered with JNK/NF-κB signaling and dose-dependently prevented ERK and p38 activation. In addition, **23** and **26** exhibited a significant protection against LPS-induced death and were able to block high glucose-activated cytokine profiles in macrophages. Together, these data show a series of anti-inflammatory chalcones with potential therapeutic effects in inflammatory diseases.

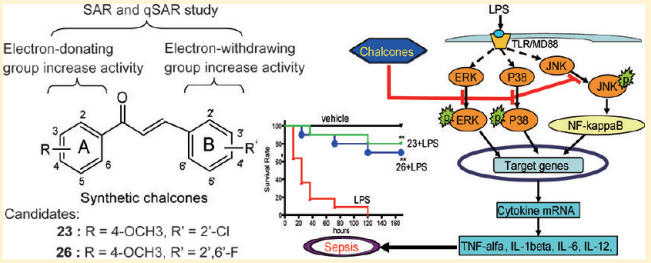

1. INTRODUCTION

It has been demonstrated that proinflammation has an association with pathophysiology and is connected with various clinical disease manifestations.[1,2] Several dominant proinflammatory cytokines, such as interleukin 6 (IL-6) and tumor necrosis factor α (TNF-α), are involved in the pathogenesis of cardiovascular and neurodegenerational diseases and cancers through a series of cytokine signaling pathways.[3,4] Overexpression of cytokines in both mRNA and protein levels is responsible for a number of pathological conditions like ulcerative colitis, diabetes, atherosclerosis, stroke, Alzheimer's disease, and cancer.[3−5] Several cytokines, such as TNF-α, IL-6, and IL-1β, have received a considerable amount of attention as molecular targets for the treatment of diseases mentioned above. The inhibition of cytokines, particularly TNF-α, has been successful in several clinical trials for the treatment of cancer and rheumatoid arthritis.[6,7] In addition, it is believed that mast cells, neutrophils, and macrophages which secrete inflammatory factors are the important players in inflammatory disorders. Inhibition of release of cytokines in activated macrophages has become a focus of current drug discovery and development and an important method for evaluating the bioactivity of drugs.[8,9]

Chalcones (Figure 1), as a group of naturally occurring compounds that belong to the flavonoid family, are present in a variety of plant species, including fruits, vegetables, spices, tea, and soy based foodstuff. Many studies have shown that naturally occurring hydroxychalcones are of great chemical and pharmacological interest, since they exhibit many biological activities, such as antifungal, antiviral, antibacterial, antimalarial, antinociceptive, anti-inflammatory, and antitumoral.[10−13] Recent reports indicate the importance of chalcones as anti-inflammatory agents involved in inhibition of cell migration and inhibition of TNF-α production in mouse model.[14] Chalcones are also excellent leading skeletons for modification of drug design and development. During the past decade, synthetic modifications of chalcones to enhance their bioactivities and to develop better therapeutic candidates have been intensively studied.[12−15] A lot of literature is available describing the role of chalcones and related derivatives as excellent anticancer, anti-inflammatory, antimitotic, antibacterial, therapeutic cardiovascular, and antihyperglycemic agents.[12−15] Recent findings suggested that some chalcones, such as the promising anti-inflammatory agents, exhibit their potential in the therapy of inflammatory and immune diseases.[14−16]

Chalcone derivatives have been extensively reported to inhibit NO synthesis and inducible NO synthetase (iNOS) and cycloxygenase 2 (COX-2) protein expression in lipopolysaccharide (LPS) stimulated cells.[13,15] The structure−activity analysis demonstrated that chalcones with substituents that reduce the electronic density in the B ring, such as chlorine atoms or nitro groups, show better biological activity and selectivity in the inhibition of nitrite production, and position 2 in B ring seems to be more important.[13,17] Regarding to the

Received: July 17, 2011
Published: October 11, 2011

   dx.doi.org/10.1021/jm200946h | J. Med. Chem. 2011, 54, 8110−8123

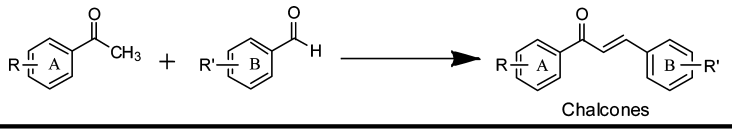

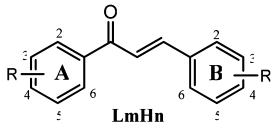

Comp.	R in A-ring	R' in B-ring	Comp.	R in A-ring	R' in B-ring
1	H	4'-$N(CH_3)_2$	28	4-OCH_3	2',4',6'-OCH_3
2	H	4'-OCH_3	29	4-OCH_3	2',4'-OCH_3
3	H	4'-OH	30	4-OCH_3	2',3'-OCH_3
4	H	2',4',6'-OCH_3	31	4-OCH_3	2'-CF_3
5	H	2',4'-OCH_3	32	4-OCH_3	2'-Br
6	H	2'-CF_3	33	4-OCH_3	3',4'-Cl
7	4-NH_2	2',4'-Cl	34	4-OCH_3	3',4'-F
8	4-NH_2	4'-$N(CH_3)_2$	35	2-OH	2',4'-Cl
9	4-NH_2	2'-Cl	36	2-OH	4'-OCH_3
10	4-NH_2	4'-OCH_3	37	2-OH	2',4',6'-OCH_3
11	4-NH_2	2'-F	38	2-OH	2',4'-OCH_3
12	4-NH_2	2',4'-OCH_3	39	3,4-F	2',4'-OCH_3
13	4-NH_2	2'-OCH_3	40	3,4,5-OCH_3	4'-$N(CH_3)_2$
14	4-NH_2	2',3'-OCH_3	41	3,4,5-OCH_3	2',4'-OCH_3
15	4-NH_2	2'-CF_3	42	3,4-OCH_3	2',4'-Cl
16	4-NH_2	2'-Br	43	3,4-OCH_3	3'-OCH_3, 4'-OH
17	3-NH_2	4'-$N(CH_3)_2$	44	3,4-OCH_3	4'-$N(CH_3)_2$
18	3-NH_2	4'-OCH_3	45	3,4-OCH_3	2'-Cl
19	3-NH_2	2',3'-OCH_3	46	3,4-OCH_3	4'-OCH_3
20	4-OCH_3	2',4'-Cl	47	3,4-OCH_3	2',4'-OCH_3
21	4-OCH_3	4'-$N(CH_3)_2$	48	3,4-OCH_3	2',3'-OCH_3
22	4-OCH_3	3'-OCH_3, 4'-OH	49	3,4-OCH_3	2'-Br
23	4-OCH_3	2'-Cl	50	3,5-F	4'-$N(CH_3)_2$
24	4-OCH_3	4'-OCH_3	51	3,5-F	3'-OCH_3, 4'-OH
25	4-OCH_3	2'-F	52	3,5-F	4'-OCH_3
26	4-OCH_3	2',6'-F	53	3,5-F	2',4'-OCH_3
27	4-OCH_3	4'-OH	54	3,5-F	2'-OCH_3

Figure 1. Structural skeleton and chemical structures of synthesized chalcones.

inhibition of inflammatory cytokines, 2′-hydroxychalcones were shown to inhibit TNF-α synthesis in mouse.[18] Recently, Bandgar et al reported the synthesis and evaluation of a series of 2-hydroxy β-chlorovinylchalcones as inhibitors of TNF-α and IL-6 in THP-1 cells.[19] However, few endeavors were proposed on evaluating the inhibitory effect of chalcone derivatives against TNF-α and IL-6 expression or their structure−activity relationship.

In this study, a series of chalcones were designed and synthesized. We evaluated the inhibitory effect of 54 synthetic chalcone derivatives against TNF-α and IL-6 production in LPS-stimulated macrophages and discussed their structure−activity relationships. A quantitative structure−activity analysis was carried out to determine the relationship between their structures and pharmacological effects. Further, active chalcones were selected for the study of anti-inflammatory mechanism at the transcriptional level. Finally, compounds **23** and **26** exhibited significant therapeutic effects against LPS-induced shock in mouse models, suggesting their potential to serve as new anti-inflammatory agents.

2. RESULTS

2.1. Synthesis of 54 Chalcones. In the present investigation, substituted chalcones were prepared by the Claisen−Schmidt condensation of substituted 1-phenylethanone and substituted benzaldehyde with NaOH as base in high yield by a known literature method.[16−19] All chalcones were prepared from the corresponding reactants. The purity was determined by TLC, and the products were characterized by analysis and comparison of their spectral and physical data including ^{1}H NMR and ESI-MS. The synthetic profiles of the compounds and their chemical structures are listed in Figure 1. The synthetic yields, melting points, ^{1}H NMR and ESI-MS results of novel and unpublished compounds are described in Experimental Section. Before use in biological experiments, compounds were recrystallized from $CHCl_3$/EtOH and HPLC was used to determine their purity (≥96.4%).

2.2. Inhibition of the LPS-Induced TNF-α and IL-6 Production by 54 Chalcones. LPS, a major component of the outer membrane of Gram-negative bacteria, acts as the prototypical endotoxin, as it binds to the Toll-like receptor 4 (TLR4) and promotes the secretion of proinflammatory cytokines in many cell types, especially in macrophages.

dx.doi.org/10.1021/jm200946h | J. Med. Chem. 2011, 54, 8110−8123

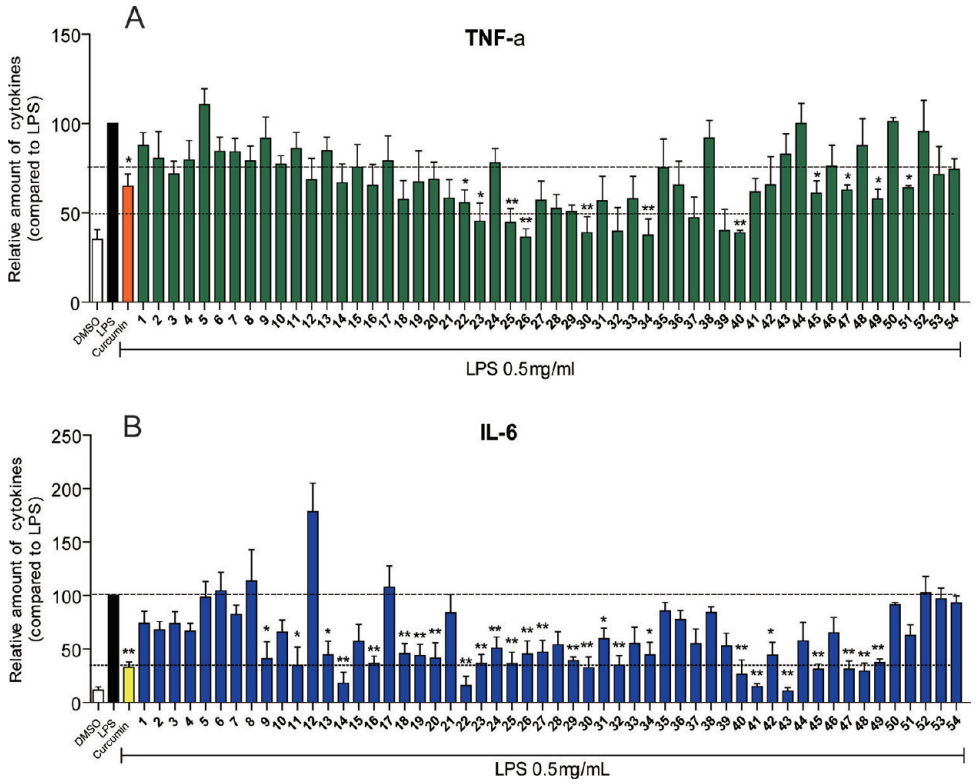

Figure 2. Synthetic chalcones inhibited LPS-induced TNF-α and IL-6 secretion in RAW 264.7 macrophages. Macrophages were plated at a density of 1.2×10^6/plate for overnight at 37 °C and in 5% CO_2. Cells were pretreated with chalcones (10 μM) for 2 h, then treated with LPS (0.5 μg/mL) for 22 h. Curcumin was used as a positive control. TNF-α and IL-6 levels in the culture medium were measured by ELISA and were normalized by the total protein. The results were presented as the percent of LPS control. Each bar represents the mean ± SD of three independent experiments. Statistical significance relative to the LPS group is indicated: *, $p < 0.05$; **, $p < 0.01$.

Hence, all 54 synthesized compounds were evaluated for anti-inflammatory activity against TNF-α and IL-6 release in LPS-stimulated mouse RAW264.7 macrophages. Cells were pretreated with compounds for 2 h and then incubated with LPS for 22 h. The amounts of TNF-α and IL-6 in culture medium were detected by enzyme-linked immunosorbent assay (ELISA) and normalized by protein concentration of cells harvested in the homologous cultural plates. The concentration at which the anti-inflammatory screening of these analogues was conducted was selected as 10 μM according to previous publications. Results are shown in Figure 2. Curcumin, a natural compound that has been extensively reported as nonsteroidal anti-inflammatory agent, was used as a reference standard for assay.

The initial screening showed that the majority of these derivatives inhibited the LPS-induced expression of TNF-α and IL-6 and especially against IL-6 expression. Twenty-five compounds exhibited 50−90% inhibition rate at a dosage of 10 μM. Their inhibitory abilities were comparable to or more pronounced than that of curcumin at the same concentration. Among these compounds, 22 compounds were found to be more potent than curcumin in inhibiting LPS-induced TNF-α expression (35−64% inhibition) and 9 compounds showed better inhibitory effects than curcumin on LPS-induced IL-6 expression (67−90% inhibition). Compounds **22**, **30**, **40**, **41**, **45**, and **47** exhibited stronger inhibition effect against both TNF-α and IL-6 expression than curcumin did. **40**, a chalcone substituted by 3,4,5-OCH_3 on the A ring and 4′-$N(CH_3)_2$ on the B ring, showed the strongest inhibitory effect on LPS-induced TNF-α and IL-6 production among tested analogues, and its inhibitory rates reached 61.2% (TNF-α) and 73.4% (IL-6).

2.3. Quantitative Structure−Activity Relationships of These Chalcones. To demonstrate the structure−activity relationship (SAR) and to evaluate the effects of various substituents on the bioactivity, a quantitative SAR (QSAR) was calculated on 54 synthetic chalcones. Monovariable and multivariable regressions between the different bioactivities, and the abundant descriptors were studied. The concrete description for QSAR study is shown in Supporting Information, and the descriptors studied here are listed in Table S1. The statistically significant models with three variables were derived for anti-IL-6 activities (eq 1 and eq 2 in Figure 3). However, no statistically significant correlation between anti-TNF-α activities and the molecular descriptors was obtained.

Equation 1 is the best QSAR model using the GETAWAY descriptors. It has a high adjusted squared regression coefficient ($R^2_{adj} = 0.72$) and is able to describe more than 74% of variances in the experimental activity. The variables in model 1 only contain the geometrical molecular descriptors. R-GETAWAY descriptors can be calculated with different atomic weightings, such as van der Waals volume, electronegativity, atomic mass, and polarizability. R-GETAWAY1 (weighted by atomic van der Waals radii) and R-GETAWAY2 (weighted by atomic Sanderson electronegativity radii) were proposed by Consonni.[20] R-GETAWAY1 and R-GETAWAY2 have the opposite influence in this model. The anti-inflammatory activities of these chalcones were regulated by R-GETAWAY1 positively and by R-GETAWAY2 negatively. The third variable,

dx.doi.org/10.1021/jm200946h | J. Med. Chem. 2011, 54, 8110−8123

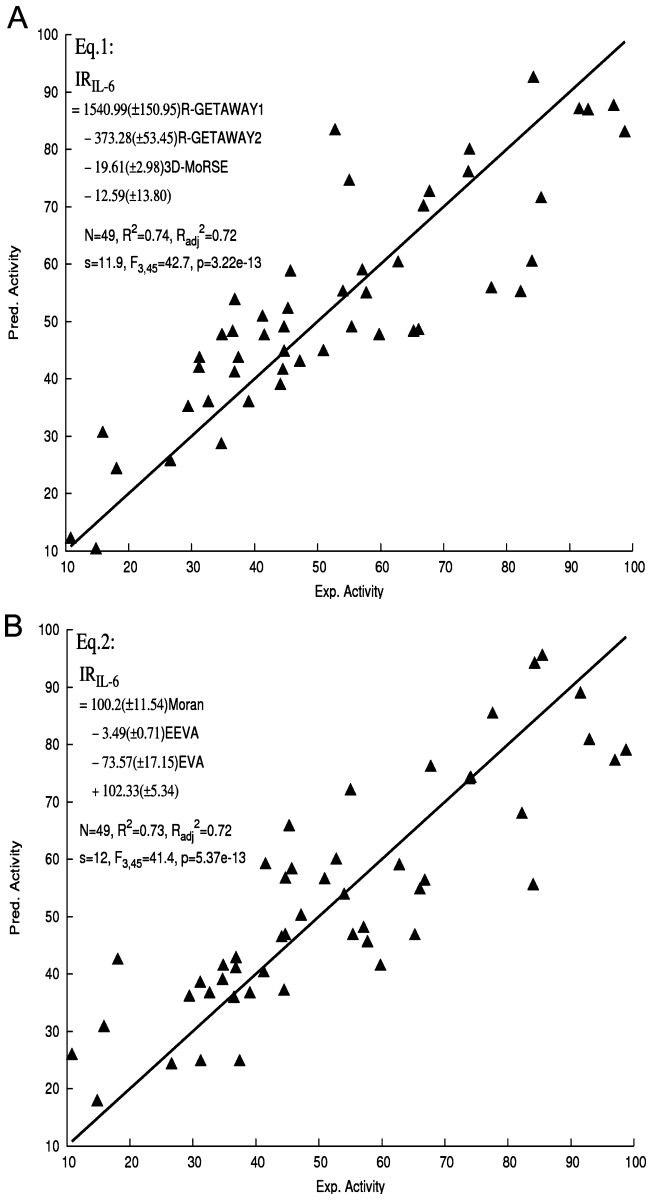

Figure 3. Plot of predicted activity against the corresponding experimental activity: *N*, the number of compounds taken into account in the regression; R^2, the multiple correlation coefficient; R_{adj}^2, adjusted multiple correlation coefficient; *s*, residual standard error; *F*, related to the *F*-statistic analysis (Fischer test). The numbers in parentheses mean the standard deviation of the coefficients.

3D-MoRSE descriptor, reflects 3D molecule structure information based on electron diffraction.[21] R-GETAWAY2 weights are dependent on the atomic Sanderson electronegativity radii, and the correlation coefficient between R-GETAWAY2 and IR_{IL-6} was obtained as 0.635. Therefore, the electronegativity may play an important role in the anti-IL-6 activity of chalcones.

Attempts were also made to construct linear models with other descriptors. Despite its squared regression coefficient (R^2 = 0.73) being close to that of eq 1, the variables in model 2 were completely different from those of model 1. Quantum chemistry descriptors and topological indices were employed to construct model 2. The EVA descriptor (eigenvalue descriptors), which was sensitive to 3D structure, was derived from fundamental mid- and near-infrared range molecular vibrational frequencies, representing a fundamental molecular property of potential energy function.[22] EEVA descriptors (electronic eigenvalue descriptors) were vector descriptors proposed as a modification of EVA. Semiempirical molecular orbital energies, such as the eigenvalues of the Schrödinger equation, are used instead of the vibrational frequencies of the molecule.[22] The scatter plot of predicted versus experimental values is illustrated in Figure 3. Equations 1 and 2 have modest quality, and the variables used in these equations may explain the variance in the IL-6-inhibitory activities of chalcone derivatives.

2.4. Active Compounds Inhibited the TNF-α and IL-6 Production in a Dose-Dependent Manner. Among tested compounds, the most promising compounds **22**, **23**, **26**, **40**, and **47** were selected for further assessment of their dose-dependent inhibitory effects against LPS-induced TNF-α and IL-6 release, and their IC_{50} was determined. RAW264.7 macrophages were pretreated with compounds at a series of concentrations (2.5, 5.0, and 10 μM) for 2 h and were subsequently incubated with LPS (0.5 μg/mL) for 22 h. The release of TNF-α and IL-6 was determined by ELISA. The results are shown in parts A and B of Figure 4, indicating a dose-dependent inhibition of LPS-induced TNF-α and IL-6 release by these analogues. Accordingly, their IC_{50} values were determined and all of them were under 10 μM except that of **22** against IL-6 release. **22** and **47** exhibited the lowest IC_{50} values against the expression of TNF-α (2.76 μM) and IL-6 (2.70 μM), respectively. Inhibition of TNF-α and IL-6 release by these compounds in a dose-dependent manner suggests their potential as anti-inflammatory agents.

2.5. Active Compounds Inhibited LPS-Induced mRNA Expression of Inflammatory Genes. To demonstrate the inhibitory effects of five active compounds against inflammatory mediators at the level of mRNA, we next determined their effects on inflammatory gene mRNAs by real-time quantitative PCR (RT-qPCR) in macrophages. Here, close to the pathological practice, we used the mouse primary mouse peritoneal macrophages (MPMs) instead of the macrophage cell line RAW264.7. Briefly, primary macrophages were treated with compounds (10 μM) and LPS (0.5 μg/mL) and total RNA was extracted. Specific mRNAs were detected by RT-qPCR. Figure 4C showed that LPS (0.5 μg/mL) increased the mRNA expression of TNF-α and IL-6 16.8- and 29.8-fold over that in vehicle-treated macrophages, respectively. When cells were pretreated with these five chalcones at 10 μM, increases of the inflammatory mRNA levels were prevented in different extents, indicating that these compounds have inhibitory effects on TNF-α and IL-6 mRNA expression.

Besides TNF-α and IL-6 evaluated above, IL-1β, IL-12, and cyclooxygenase 2 (COX-2) have been demonstrated as inflammatory mediators that play important roles in inflammation and various related diseases.[23,24] Thus, we determined whether these five compounds have any inhibitory effects on the mRNA expression of IL-1β, IL-12, and COX-2 after treatment with compounds and LPS as mentioned above. As shown in parts C and D of Figure 4, LPS significantly increased the level of the mRNAs of IL-1β, IL-12, and COX-2 compared to those of the vehicle control. Except for the inhibitory effects of **26** (against COX-2) and **40** (against COX-2 and IL-1β) that were not statistically significant, the majority of these chalcones potently inhibited LPS-induced up-regulation of IL-1β, IL-12, and COX-2 transcripts with a statistical significance ($p < 0.05$ or $p < 0.01$) in macrophages. These data suggest that chalcones affect the cytokine profile partly at the level of mRNA.

dx.doi.org/10.1021/jm200946h | J. Med. Chem. 2011, 54, 8110–8123

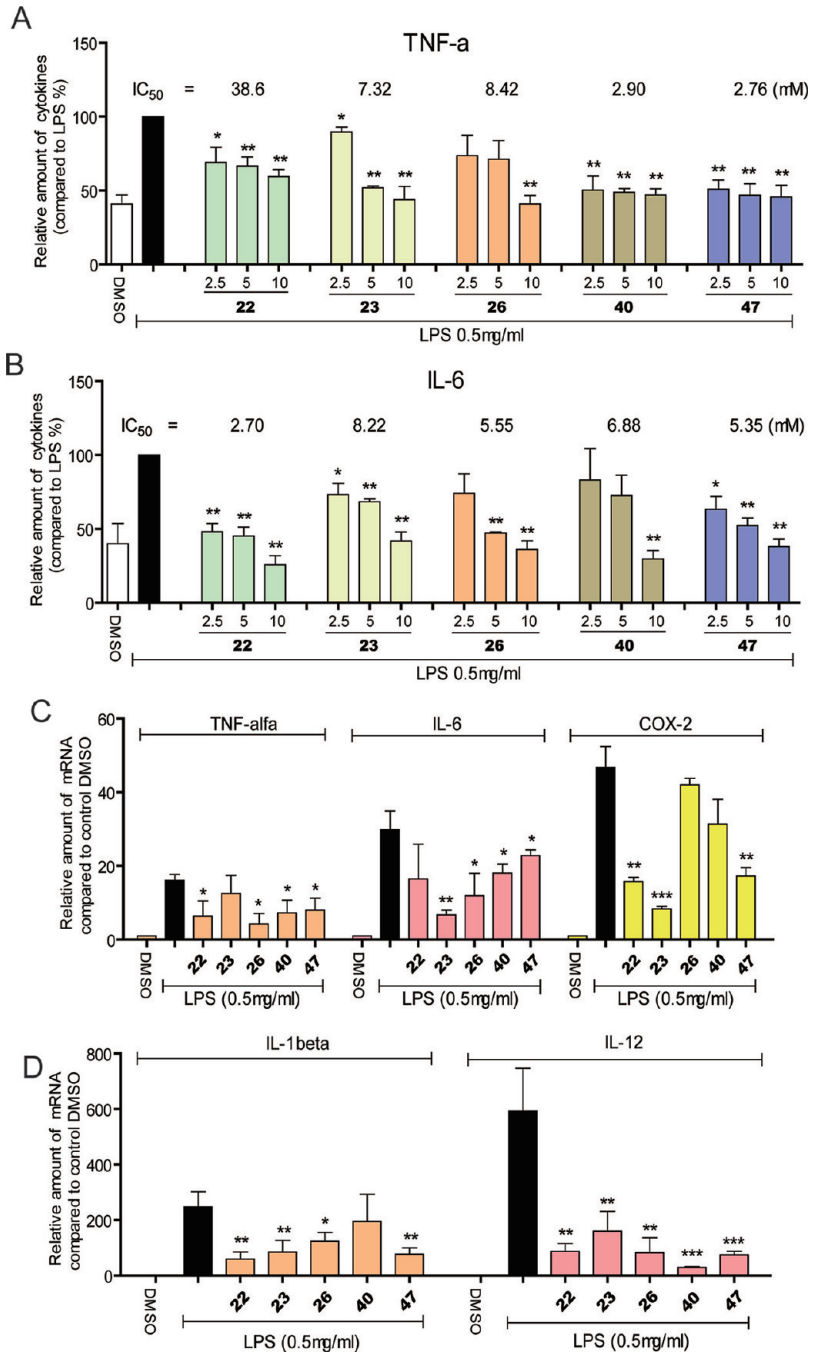

Figure 4. Five active chalcones inhibited LPS-induced TNF-α and IL-6 release in a dose-dependent manner in RAW 264.7 macrophages. (A, B) Macrophages were plated at a density of 1.2×10^6/plate overnight at 37 °C and in 5% CO_2. Cells were pretreated with specific compound at indicated concentrations for 2 h, followed by LPS (0.5 μg/mL) treatment for 22 h. TNF-α (A) and IL-6 (B) levels in the culture medium were measured by ELISA and were normalized to the total protein amount. The results are expressed as percentage of LPS control. (C, D) Cells were pretreated with compounds at 10 μM or vehicle control for 2 h and treated with LPS (0.5 μg/mL) for 6 h. The mRNA levels of inflammatory mediators TNF-α, IL-6, COX-2, IL-1β, and IL-12 were quantified by RT-qPCR. The mRNA values for each gene were normalized to internal control β-actin mRNA and were expressed as a ratio to DMSO. Each bar represents the mean ± SD of four to seven independent experiments. Statistical significance relative to LPS group is indicated: *, $p < 0.05$; **, $p < 0.01$.

2.6. Compounds 23 and 26 Suppress the LPS-Induced JNK/NF-kB Signaling in MPMs. LPS signal transduction has been shown by other researchers to activate a variety of signal pathways, including the NF-κB pathway, which controls the transcription of a number of inflammatory cytokines.[25,26] Some chalcones have been identified as an inhibitor for NF-κB-dependent inflammation.[13,15,27] In NF-κB signaling, IκB degradation frees NF-κB p65 subunit from sequestration, allowing it to translocate to the nucleus, bind to target promoters, and turn on transcriptions of inflammatory genes including TNF-α, IL-6, IL-1β, IL-12, and COX-2. We next determined the effects of two representative compounds, **23** and **26**, on IκB degradation and NF-κB p65 translocation from cytoplasma to nuclei. As shown in Figure 5A–D, LPS could strengthen NF-κB p65 nuclear translocation (red point in blue nucleus), while in **23**- and **26**-pretreated macrophages,

dx.doi.org/10.1021/jm200946h | J. Med. Chem. 2011, 54, 8110–8123

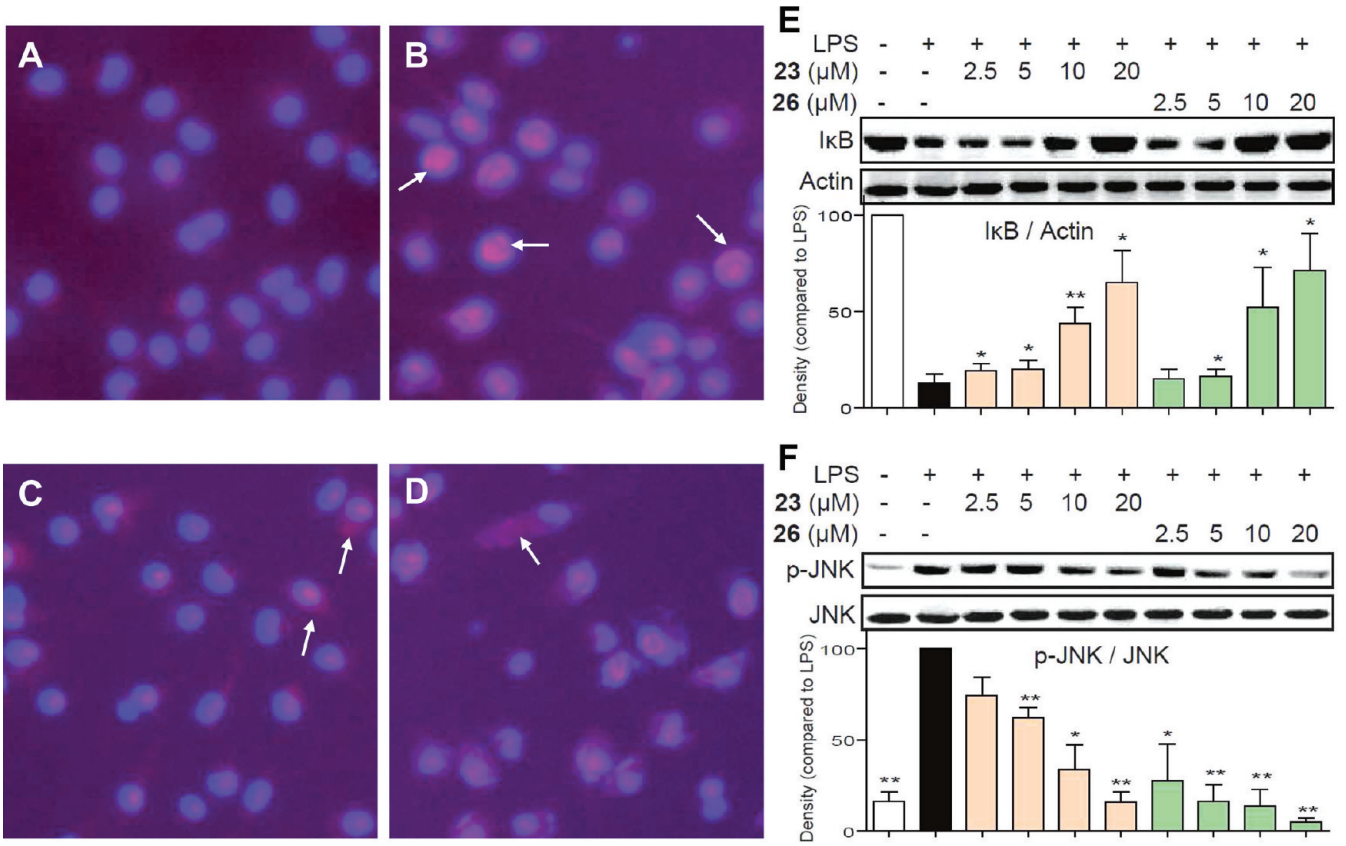

Figure 5. Active chalcones **23** and **26** inhibited LPS-induced JNK/NF-κB signaling activation. (A–D) Cultured MPMs were pretreated with vehicle (DMSO) or 10 μM compound (**23** or **26**) for 2 h and then stimulated with 0.5 μg/mL LPS. After 1 h of treatment, the cells were incubated with p65 antibody and Cy3 fluorescein-conjugated secondary antibody, and nuclei were stained with DAPI. The images (200×) were obtained by fluorescence microscope and overlay: (A) vehicle control group; (B) LPS alone group; (C) LPS + **23** group; (D) LPS + **26** group. Similar results were obtained with five independent experiments. (E, F) MPMs were pretreated with vehicle (DMSO), **23**, or **26** (at 2.5, 5, 10, or 20 μM) for 2 h and then stimulated with LPS (0.5 μg/mL) for 30 min. The levels of IκBα (E) and p-JNK (F) were examined using specific antibodies with actin and JNK as the loading control, respectively. The column figures show the normalized optical density as a percentage of control group. Bars represent the mean ± SEM of three independent experiments: (*) $p < 0.05$, (**) $p < 0.01$, vs LPS alone group.

LPS-induced nuclear p65 decreased, suggesting that **23** and **26** inhibited p65 translocation from cytophasma to nuclei. Figure 4E demonstrated that LPS increased IκB degradation after 30 min of incubation, whereas pretreatment with **23** and **26** (2.5, 5, 10, and 20 μM) dose-dependently reversed LPS-induced IκB degradation. JNK has been established as a key transcriptional regulator of inflammatory cytokines and an upstream coregulator of NF-κB signaling. The data in Figure 4F further showed that **23** and **26** (2.5, 5, 10, and 20 μM) also dose-dependently inhibited LPS-induced JNK phosphorylation in macrophages. These results suggest that the anti-inflammatory activity of active chalcones **23** and **26** may be associated with its negative effects on JNK/NF-κB activation.

2.7. Active Compounds Suppressed the LPS-Induced MAPK Activation in MPMs. The phosphorylations of mitogen-activated protein kinases (MAPKs), expecially extracellular signal-regulated kinase (ERK) and p38 kinase, have also been implicated to induce cytokine expression in response to various inflammatory stimuli containing LPS.[26,28] Thus, we hypothesized that these five compounds interfered with the phosphorylation of ERK or p38 kinases. As shown in parts A and B of Figure 6A, LPS incubation for 20 min elevated the phosphorylation levels of ERK and p38 while pretreatment with these five compounds at 10 μM significantly decreased LPS-dependent ERK and p38 phosphorylation in mouse macrophages ($p < 0.05$ or $p < 0.01$). Only L6H3 pretreatment did not exhibit a statistically significant alteration ($p > 0.05$) against p38 activation.

Furthermore, Figure 6C revealed that **23**, at 2.5, 5.0, 10, and 20 μM, is able to inhibit LPS-induced ERK and p38 phosphorylation in macrophages in a dose-dependent manner. In Figure 6D, **26** also demonstrated a dose-dependent inhibition against p38 phosphorylation. Although the concentration of 5.0 μM did not match a dose-dependent manner, **26** at four concentrations still exhibited strong effects on LPS-induced ERK activation. In particular, at a dosage of 20 μM, these two compounds almost completely blocked ERK and p38 activation. Therefore, these results indicate that ERK and p38 phosphorylation might be an important step in mediating anti-inflammatory effects of these chalcones in macrophages.

2.8. Effect of 23 and 26 Pretreatment on Survival Rate in Mice after LPS administration. To determine whether **23** and **26** are able to attenuate endotoxin shock through inhibition of LPS-induced inflammatory response, 15- to 18-week-old mice were injected with LPS at a dosage of 20 mg/kg intrapenitoneally in the presence or absence of **23** and **26** treatment and their survival rates were monitored for 7 days. As shown in Figure 7A, all animals treated with LPS alone died within 5 days as a result of the septic shock. In animals receiving compounds at 15 mg/kg prior to LPS treatment, the

dx.doi.org/10.1021/jm200946h | J. Med. Chem. 2011, 54, 8110–8123

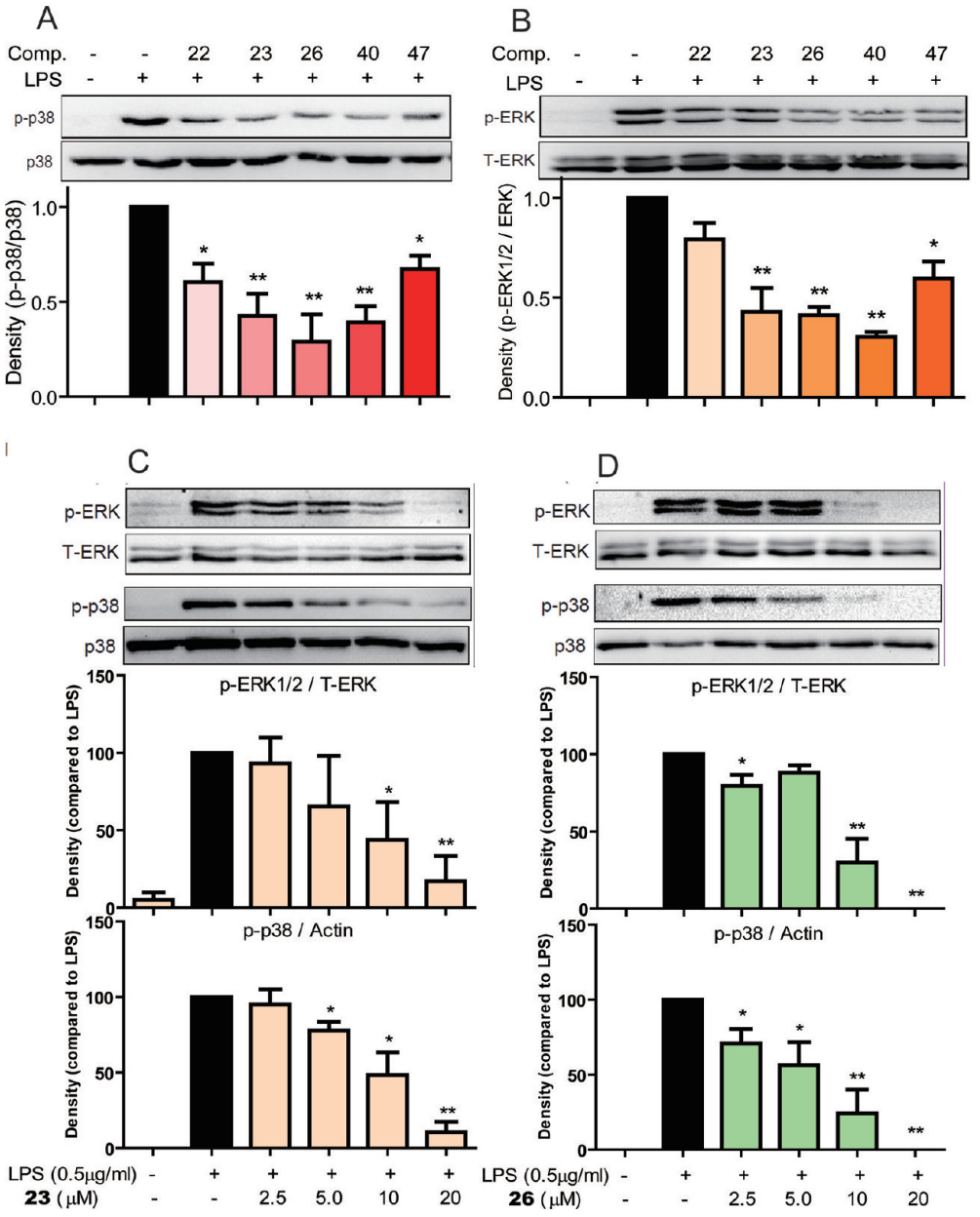

Figure 6. Active chalcones inhibited LPS-induced ERK and p38 phosphorylation. Macrophages were pretreated with vehicle (DMSO) or indicated compounds at indicated concentrations for 2 h followed by incubation with LPS (0.5 μg/mL) for 1 h. The protein levels of p-ERK, ERK, p-p38, and p38 were examined by Western blot with actin as a loading control: (A, B) five active chalcones at 10 μM; (C) **23** at indicated concentrations; (D) **26** at indicated concentrations. The column figures represent the optical density ratio. Each bar represents the mean ± SE of three independent experiments: (*) $p < 0.05$, (**) $p < 0.01$, vs LPS group.

survival rates were significantly increased compared to that of the control group (70% and 80% survival in **23**-treated group and **26**-treated group, respectively, $p < 0.001$ in both groups vs LPS group). Meanwhile, the body weight of L6H4- and L6H9-treated mice decreased during 0−60 h but regained slowly 60 h after LPS treatment (Figure 7B). Thus, pretreatment of **23** or **26** prolonged survival in LPS-induced acute inflammatory model.

2.9. Active Compounds Inhibited the High Glucose-Induced Inflammatory Gene Transcription in MPMs.

Besides LPS, a lot of stimuli, such as high glucose (HG), have been reported to activate cellular NF-κB signaling, resulting in the release of a large amount of inflammatory cytokines and promoting chronic inflammation and tissue destruction.[29,30] We next examined whether these five active chalcones could alter HG-induced inflammatory gene expression. MPMs were pretreated with compounds or vehicle for 2 h, followed by HG incubation for 3 h. The mRNA expression was measured using RT-qPCR in the whole cell RNA extracts. The results in Figures 7C−F show that HG induced an evident increase in the mRNA expression of proinflammatory cytokines, including TNF-α, IL-1β, IL-12, and IL-6. The five chalcones at 10 μM significantly decreased the HG-induced inflammatory mRNA expression compared to the HG-treated group expect for **40** against IL-6 and **47** against IL-1β. These data indicate that active chalcones are also potent inhibitors for HG-induced inflammatory gene mRNA overexpression in MPMs. They have

dx.doi.org/10.1021/jm200946h | J. Med. Chem. 2011, 54, 8110−8123

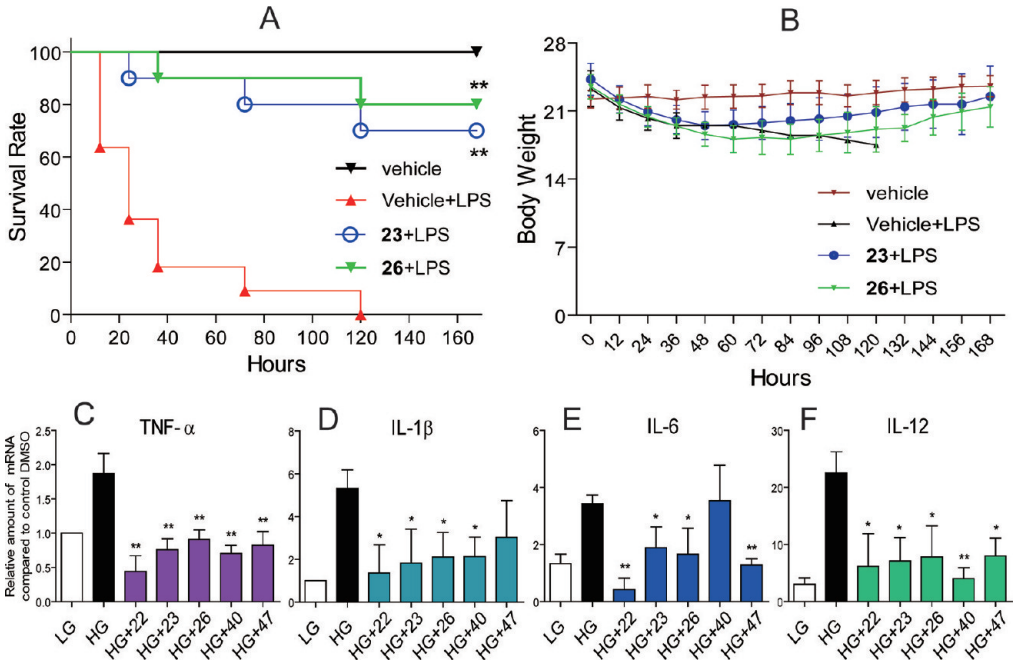

Figure 7. Active chalcone derivatives inhibited LPS- and HG-induced inflammation. (A, B) Mice were pretreated with vehicle (saline) or 15 mg/kg **23** or **26** (iv) 15 min before the injection of 20 mg/kg of LPS (iv). Survival (A) and body weight (B) were recorded for 7 days after the LPS injection at an interval of 12 h: $n = 10$ animals in each group; (**) $p < 0.01$ vs LPS group. (C–F) MPMs (1×10^6) were pretreated with indicated compounds (10 μM) or vehicle (DMSO) for 2 h and then stimulated with HG (25 mM glucose) for 3 h. Cells in the low glucose (LG) group were cultured in RPMI-1640 medium containing 5.5 mM glucose. The mRNA levels of TNF-α (C), IL-1β (D), IL-6 (E), and IL-12 (F) were detected by the RT-qPCR method as described in Experimental Section. Bars represent the mean ± SEM of three independent experiments performed in duplicate, and asterisks indicate significant inhition: (*) $p < 0.05$, (**) $p < 0.01$, vs HG group.

the potential to be used for diabetic complications, which are partly mediated by hyperglycemia-induced inflammation.

3. DISCUSSION

The main findings of this study are that we have developed novel chalcones with potent anti-inflammatory activities and they are able to be developed as therapeutic agents for inflammatory diseases. Nonsteroidal anti-inflammatory drugs (NSAIDs) are therapeutically important in the treatment of rheumatic arthritis and various types of inflammatory conditions but found to be limited in clinical applications because of their gastrointestinal side effects.[31] Chalcone is a unique template that is associated with several biological activities, especially anti-inflammatory and anticancer activities. The convenience of preparation, the potential of oral administration, and the safety also support the feasibility of chalcone-based compounds as therapeutic agents. Tremendous effort has been devoted to elucidate the mechanisms of chalcone-based compounds for their promising biological activities, including their immunomodulation and interference in cellular signaling pathways, such as NF-κB inhibition.[12−16]

A few chalcone-based compounds have been reported to alter the cytokine profiles.[14] Interestingly, these chalcone-based cytokine inhibitors possess diverse structural properties with varied substitutions, most of which are electron donating functionalities, such as hydroxy and methoxy functional groups, at different positions of both aromatic systems.[15,16] In addition, a number of naturally occurring chalcones are polyhydroxylated in the aryl rings. The radical quenching properties of the phenolic groups may contribute to the antioxidant and anti-inflammatory benefits of chalcones.[32,33] It is therefore important to elucidate the structural requirements for chalcone-based compounds with respect to anti-inflammation to determine whether potent and easily accessible chalcones can be developed for future therapeutic evaluation. In the present study, 54 chalcones were synthesized and evaluated for the inhibitory activities against LPS-induced TNF-α and IL-6 release in macrophages. Many of these chalcones are easily obtainable through one-step aldol condensation. According to bioscreening results against IL-6, it may be beneficial to the inhibitory effect when electron-donating substitutes were positioned in ring A, while electron-withdrawing groups in ring B may contribute to a better bioactivity to these chalcones. Generally, the activities may be ordered as follows: compounds **40** and **41** (with 3,4,5-OCH_3 in ring A) and **42−49** (3,4-OCH_3) > **20−34** (4-OCH_3) > **7−16** (4-NH_2) and **17−19** (5-NH_2) > **35−38** (2-OH) > **1−6** (H) > **50−54** (3,5-F). In ring B, where the effect of electron negativity on IL-6 inhibition is not as obvious as that in ring A, the existence of an electron-withdrawing halogen markedly increased the inhibitory activity of chalcones. However, it is difficult to obtain the SAR of chalcones in TNF-α inhibition based on the data we got in this study.

Similar conclusions were drawn by a quantitative SAR calculation. As can be seen, eq 1 has a modest quality and the variables used in these equations can explain the variance in the anti-IL-6 activities of chalcone derivatives. In spite of the similar R^2 they have, the correlation between compound activities and structure information could be illustrated from different perspectives by using various descriptors. To test the validity of the models, the q^2 values were adopted as a measure of the predictive ability of a regression equation, which was the square of the correlation coefficient of the cross-validation and was calculated from the leave-one-out (LOO) test. R^2 was a

dx.doi.org/10.1021/jm200946h | J. Med. Chem. 2011, 54, 8110−8123

common parameter to test the validity of models, while it could be increased artificially by adding more variables (descriptors). In contrast, q^2 was a more reliable statistic parameter. The q^2 values of eqs 1 and 2 were 0.71 and 0.70, respectively, indicating the stability and reliability of these models.

TNF-α and IL-6 play pivotal roles in several inflammatory conditions.[3−5] The inhibition of TNF-α and IL-6 release by **22**, **23**, **26**, **40**, and **47** in a dose-dependent manner (parts A and B of Figure 4) confirms the bioscreening results and demonstrates their potential to be developed as anti-inflammatory agents. Upon stimulation with LPS, the various inflammatory mediators such as cytokines and enzymes are induced at varying magnitudes and at different time points.[23,24] The mRNA levels of IL-1β, IL-12, and COX-2 were all shown to be up-regulated by LPS treatment. Five compounds significantly reduced the production of TNF-α, IL-6, IL-1β, IL-12, and COX-2 at the transcription level, further establishing their anti-inflammatory properties. The fact that **26** and **40** did not decrease LPS-raised COX-2 mRNA levels and the difference in mRNA fold change of some cytokines between treated cells with different chalcones may reveal a mechanistic diversity at the transcriptional or posttranscriptional level among these chalcones (parts C and D of Figure 4).

MAPKs (ERK, JNK, and p38) have received increasing attention as a target molecule for inflammatory response including macrophage activation and cytokine release.[26,28] In response to LPS stimulation, JNKs are activated via phosphorylation and then lead to the activation of NF-κB.[28,34] The phosphorylation of ERK and p38 MAPK increases the cytokine gene expression through direct transcriptional regulation. A lot of drugs that modulate the activity of MAPK pathways have shown promise for treating chronic inflammatory diseases. Recently, three natural chalcones, kurarinone,[35] kuraridin,[35] and panduratin A,[36] are reported to be able to suppress the LPS and UV-induced inflammation by inhibiting the activation of JNK, ERK, and p38 pathways. In this study, we demonstrated that the effects of five active chalcones inhibit ERK and p38 phosphorylation to different extent in LPS-stimulated primary macrophages (parts A and B of Figures\s 6). Also, the representative **23** and **26** showed dose-dependent inhibition against JNK (Figure 5F), ERK (Figure 6C), and p38 activation (Figure 6D). These results suggest that the inhibition of the production of proinflammatory mediators by chalcones may occur through the down-regulation of the MAPK pathways.

It has been well accepted that the NF-κB signaling pathway plays important roles in the activation of macrophages. NF-κB is responsible for the regulation of a plethora of genes involved in carcinogenesis and inflammation. The suppression of NF-κB-mediated inflammation and cancer by some of the most significant natural chalcones, including flavokawin, butein, xanthoangelol, 4-hydroxyderricin, cardamonin, 2′,4′-dihydroxychalcone, isoliquiritigenin, isosalipurposide, and naringenin chalcone, was reviewed by Yadav et al. recently.[10] Also, 2′,4′-dihydroxy-6′-methoxy-3′,5′-dimethylchalcone was recently reported to prevent nuclear translocation of the NF-κB p65 subunit by reducing IκBα phosphorylation and degradation, which resulted in a suppression of LPS-induced inflammatory factors.[37] In this regard, we have also provided novel in vitro evidence that **23** and **26** significantly reversed IκB degradation (Figure 5E) and suppressed the NF-κB p65 translocation from cytosol to nuclei (Figure 5A−D) in LPS-stimulated macrophages, indicating that down-regulation of activity of NF-κB is involved and appears to be the possible mechanism responsible for the anti-inflammatory effects of **23** and **26**. As an upstream co-regulator of NF-κB, JNK was also inactivated by pretreatment of **23** and **26** in a dose-dependent manner. Taken together, this beneficial effect of our chalcones on macrophages is associated with the inactivation of MAPKs and NF-κB as potential targets. Additionally, p38 MAPK may also function post-transcriptionally through a change of mRNA stabilization or at the level of protein translation. It remains unknown whether the protective effect of chalcones on cytokine profile responsive to LPS is also involved the regulation of inflammatory gene mRNA stability. Further studies are also required to examine the effect of chalcones at the post-transcriptional level.

As a major endotoxin, LPS from Gram-negative bacteria has been implicated as a major cause of sepsis. Inflammatory shock as a consequence of LPS release remains a serious clinical concern, which can cause a variety of pathologies ranging from mild (fever) to lethal (septic shock, organ failure, and death).[38] A number of different approaches have been investigated to try to treat and/or prevent the septic shock associated with infections caused by Gram-negative bacteria, including blockage of one or more of the cytokines induced by LPS signaling.[39] Our data have demonstrated the inhibitory effects of chalcones on LPS-signaling events. For potential clinical application, we further confirmed that **23** and **26** would significantly decrease LPS-induced lethality (parts A and B of Figure 7). In addition, inflammation is being recognized as one of main factors in the pathogenesis of diabetic complications. Cytokines, mainly IL-12, IL-6, and IL-1β, as well as TNF-α act as pleiotropic polypeptides regulating chronic inflammatory and immune responses in the pathophysiology of a range of diseases, including diabetic complications.[29,30] Hyperglycemia-induced inflammation is involved in the development and progression of diabetic microvascular and renal complications.[40,41] We also found that these chalcones were able to block high glucose-activated cytokine profiles in macrophages (Figures 7C−F). To the best of our knowledge, this is the first time that the potential of chalcones to attenuate chronic inflammatory response caused by high glucose circumstance has been shown. Thus, our data lend support to these findings and provide novel evidence for the anti-inflammatory effects of these synthetic chalcones on a systemic scale and their potential treatment in sepsis as well as in chronic inflammatory diseases. Although the anti-inflammatory mechanism against HG-induced stress is still unknown, the beneficial effects of our synthetic chaclones on HG-induced inflammation and diabetic complications will become one of our targets in the continuing research.

In summary, these findings suggested that some chalcones may be promising anti-inflammatory agents and have potential in the therapy of septic shock. Being of natural origin, chalcone may be devoid of toxicity and hence beneficial for drug discovery as active compounds. This report described the chemistry of further synthesized chalcones, biological activity, and the structure−activity relationships of this series of anti-inflammatory agents. However, further studies are necessary to establish such notion. Such studies should include testing of these new anti-inflammatory chalcones in more animal models and examination of the underlying molecular mechanisms and direct targets at the transcriptional or post-transcriptional level.

4. EXPERIMENTAL SECTION

4.1. Chemical Synthesis. Melting points were determined on a Fisher-Johns melting apparatus and were uncorrected. ^{1}H NMR

spectra were recorded on a 600 MHz spectrometer (Bruker Corporation, Switzerland). The chemical shifts were presented in parts per million with TMS as the internal reference. Electropray ionization mass spectra in positive mode (LC−ESI-MS) data were recorded on a Bruker Esquire HCT spectrometer. Column chromatography purifications were carried out on silica gel 60 (E. Merck, 70−230 mesh). Fifty-four chalcones were synthesized by Claisen−Schmidt condensation between different substituted acetophenones and arylaldehydes. Chalcones with hydroxyl groups were synthesized by reflux in acidic medium using HCl as catalyst, while other cholcones were synthesized at 5−8 °C under NaOH condition. All the reactions were monitored by the silica gel thin layer chromatography. At the end of the reaction, water is added into the mixture to precipitate the products. Compounds **3**, **4**, **6**, **15**, **16**, **23**, **24**, **25**, **27**, **32**, **38**, **41**, **47**, **48**, and **53** were purified by recrystallization using MeOH/CH_2Cl_2. Other compounds were purified by silica gel column chromatography. The yields of products were in the range of 10−95% after purification. Their structures were characterized by spectral data from IR, MS, and ^{1}H NMR. The spectral data of novel or unreported compounds are listed as the following.

*(E)-4-(Dimethylamino)chalcone (**1**).* The product was recrystallized from ethanol/CH_2Cl_2 (1:2). Yellow crystal, 32.4% yield, mp 97.8−98.9 °C. ^{1}H NMR ($CDCl_3$) δ: 8.003 (d, J = 7.8 Hz, 2H, H-2′, H-6′), 7.793 (d, J = 15.6 Hz, 1H, H-β), 7.552 (d, J = 8.4 Hz, 2H, H-2, H-6), 7.545 (t, 1H, H-4′), 7.491 (t, 2H, H-3′, H-5′), 7.337 (d, J = 15.6 Hz, 1H, H-α), 6.698 (d, J = 8.4 Hz, 2H, H-3, H-5), 3.046 (s, 6H, $N(CH_3)_2$-4). ESI-MS m/z: 252.7 $(M + 1)^+$; calcd for $C_{17}H_{17}NO$, 251.32.

*(E)-2,4-Dimethoxyphenylchalcone (**5**).* Yellow syrup, 62.2% yield. ^{1}H NMR ($CDCl_3$) δ: 8.056 (d, J = 15.6 Hz, 1H, H-β), 8.003 (d, J = 9.0 Hz, 2H, H-2′, H-6′), 7.572 (d, J = 8.4 Hz, 1H, H-6), 7.566 (d, J = 15.6 Hz, 1H, H-α), 7.557 (t, 1H, H-4′), 7.497 (t, 2H, H-3′, H-5′), 6.533 (d, J = 8.4 Hz, 1H, H-5), 6.475 (s, J = 2.4 Hz, 1H, H-3). ESI-MS m/z: 269.0 $(M + 1)^+$; calcd for $C_{17}H_{16}O_3$, 268.31.

*(E)-2-Trifluoromethylchalcone (**6**).* Light yellow powder, 66.0% yield, mp 54.8−56.1 °C. ^{1}H NMR ($CDCl_3$), δ: 8.112 (d, J = 7.8 Hz, 2H, H-2′, H-6′), 7.738 (d, J = 8.4 Hz, 2H, H-2, H-6), 7.718 (d, J = 15 Hz, 1H, H-β), 7.698 (d, J = 15.0 Hz, 1H, H-α), 7.649 (t, 1H, H-4′), 7.559 (t, 2H, H-3′, H-5′), 6.837 (d, J = 9 Hz, 2H, H-3, H-5). ESI-MS m/z: 277.6 $(M + 1)^+$; calcd for $C_{16}H_{11}F_3O$, 276.25.

*(E)-4-(Dimethylamino)-4′-aminochalcone (**8**).* Salmon pink powder, 35.0% yield, mp 59.7−66.6 °C. ^{1}H NMR ($CDCl_3$), δ: 7.920 (d, J = 8.4 Hz, 2H, H-2′ H-6′), 7.781 (d, J = 15.6 Hz, 1H, H-β), 7.737 (d, J = 9 Hz, 2H, H-2, H-6), 7.354 (d, J = 15.6 Hz, 1H, H-α), 6.644 (d, J = 9 Hz, 2H, H-3, H-5), 6.690 (d, J = 8.4 Hz, 2H, H-3′, H-5′), 4.118 (brs, 2H, NH_2-4′), 3.058 (s, 6H, $N(CH_3)_2$-4′). ESI-MS m/z: 267.3$(M + 1)^+$; calcd for $C_{17}H_{18}N_2O$, 266.34.

*(E)-2-Chloro-4′-aminochalcone (**9**).* Yellow powder, 81.1% yield, mp 132.3−135.7 °C. ^{1}H NMR ($CDCl_3$), δ: 8.132 (d, J = 15.6 Hz, 1H, H-β), 7.926 (d, J = 8.4 Hz, 2H, H-2′, H-6′), 7.733 (d, J = 9.6 Hz, 1H, H-6), 7.490 (d, J = 15.6 Hz, 1H, H-α), 7.431 (d, J = 9 Hz, 1H, H-3), 7.307 (m, 1H, H-5), 7.302 (m, 1H, H-3), 6.700 (d, J = 8.4 Hz, 2H, H-3′, H-5′), 4.190 (brs, 2H, NH_2-4′). ESI-MS m/z: 258.3 $(M + 1)^+$; calcd for $C_{15}H_{12}ClNO$, 257.71.

*(E)-4-Methoxy-4′-aminochalcone (**10**).* Flavovirens powder, 38.2% yield, mp 139.5−144.5 °C. ^{1}H NMR ($CDCl_3$), δ: 7.928(d, J = 9 Hz, 2H, H-2′ H-6′), 7.759 (d, J = 15.6 Hz, 1H, H-β), 7.592 (d, J = 9 Hz, 2H, H-2, H-6), 7.428 (d, J = 15.6 Hz, 1H, H-α), 6.929 (d, J = 8.4 Hz, 2H, H-3, H-5), 6.702 (d, J = 9 Hz, 2H, H-3′, H-5′), 4.180 (brs, 2H, NH_2-4′), 3.92 (s, 3H, OCH_3-4′). ESI-MS m/z: 254.0 $(M + 1)^+$; calcd for $C_{16}H_{15}NO_2$, 253.3.

*(E)-2,4-Dimethoxy-4′-aminochalcone (**12**).* Yellow powder, 54.8% yield, mp 57.1−59.1 °C. ^{1}H NMR ($CDCl_3$), δ: 8.019 (d, J = 15.6 Hz, 1H, H-β), 7.917 (dd, J = 1.8 Hz, 7.2 Hz, 2H, H-2′, H-6′), 7.812 (d, J = 9.0 Hz, 1H, H-6), 7.562 (d, J = 8.4 Hz, 1H, H-5), 7.545 (d, 1H, H-α), 6.690 (dd, J = 1.8 Hz, 7.2 Hz, 2H, H-3′, H-5′), 6.472 (s, J = 1.8 Hz, 1H, H-3), 4.114 (brs, 2H, NH_2-4), 3.892 (s, 3H, OCH_3-2), 3.875 (s, 3H, OCH_3-4). ESI-MS m/z: 285.1 $(M + 1)^+$, 282.3 $(M - 1)^-$; calcd for $C_{17}H_{17}NO_3$, 283.32

*(E)-2-Methoxy-4′-aminochalcone (**13**).* Orange yellow powder, 75.0% yield. ^{1}H NMR ($CDCl_3$), δ: 8.084 (d, J = 15.6 Hz, 1H, H-β), 7.929 (d, J = 8.4 Hz, 2H, H-2′, H-6′), 7.620 (d, J = 15.6 Hz, 1H, H-α), 7.615 (d, J = 9.0 Hz, 1H, H-6), 7.345 (t, 1H, H-4), 6.984 (t, 1H, H-5), 6.934 (d, J = 9.0 Hz, 1H, H-3), 6.696 (d, J = 8.4 Hz, 2H, H-3′, H-5′), 4.190 (brs, 2H, NH_2-4′), 3.920 (s, 3H, OCH_3-2). ESI-MS m/z: 254.7 $(M + 1)^+$; calcd for $C_{16}H_{15}NO_2$, 253.3.

*(E)-2,3-Dimethoxyphenyl-4′-aminochalcone (**14**).* Orange yellow powder, 68.9% yield, mp 135.6−136.8 °C. ^{1}H NMR ($CDCl_3$), δ: 8.051(d, J = 15.6 Hz, 1H, H-β), 7.929(d, J = 8.4 Hz,2H,H-2′,H-6′), 7.602 (d, J = 15.6 Hz, 1H, H-α), 7.274(d, J = 8.4 Hz, 1H, H-6), 7.083 (t, 1H, H-5), 6.948 (d, J = 8.4 Hz, 1H, H-4), 6.700 (d, J = 8.4 Hz, 2H, H-3′, H-5′), 4.190 (brs, 2H, NH_2-4′), 3.888 (s, 3H, OCH_3-2), 3.876 (s, 3H, OCH_3-3). ESI-MS m/z: 284.1 $(M + 1)^+$; calcd for $C_{17}H_{17}NO_3$, 283.32.

*(E)-4-Dimethylamino-3′-aminochalcone (**17**).* salmon pink powder, 53.8% yield, mp 130.5−135.1 °C. ^{1}H NMR ($CDCl_3$), δ: 7.768 (d, J = 15.6 Hz, 1H, H-β), 7.536 (d, J = 8.4 Hz, 2H, H-2, H-6), 7.375 (d, J = 7.2 Hz, 1H, H-6′), 7.308 (s, 1H, H-2′), 7.287 (d, J = 15.6 Hz, 1H, H-α), 7.246−7.260 (m, 1H, H-5), 6.860 (dd, J = 2.4 Hz, 7.8 Hz, 1H, H-4′), 6.689 (d, J = 9.0 Hz, 2H, H-3, H-5), 3.811 (brs, 2H, NH_2-3′), 3.042 (s, 6H, $(CH_3)_2$N-4). ESI-MS m/z: 266.9 $(M + 1)^+$; calcd for $C_{17}H_{18}N_2O$, 266.34

*(E)-4-Methoxy-3′-aminochalcone (**18**).* Light yellow powder, 18.1% yield, mp 148.1−150.6 °C. ^{1}H NMR ($CDCl_3$), δ: 7.758 (d, J = 16.2 Hz, 1H, H-β), 7.589 (dd, J = 1.8 Hz, 6.6 Hz, 2H, H-2, H-6), 7.385 (d, J = 7.8 Hz, 1H, H-6′), 7.361 (d, J = 15.6 Hz, 1H, H-α), 7.334 (t, J = 3.62 Hz, 1H, H-2′), 7.278 (d, J = 7.8 Hz, 1H, H-5′), 6.930 (dd, J = 1.8 Hz, 7.2 Hz, 2H, H-3, H-5), 6.903 (dd, J = 1.8 Hz, 7.8 Hz, 1H, H-4′), 3.852 (s, 3H, OCH_3-4). ESI-MS m/z: 253.8 $(M + 1)^+$; calcd for $C_{16}H_{15}NO_2$, 253.3.

*(E)-2,3-Dimethoxy-3′-aminochalcone (**19**).* Light yellow powder, 57.2% yield, mp 95.4.6−96.8 °C. ^{1}H NMR ($CDCl_3$), δ: 8.141 (d, J = 15.6 Hz, 1H, H-β), 7.925 (d, J = 7.8 Hz, 1H, H-6′), 7.867 (s, 1H, H-2′), 7.786 (d, J = 7.8 Hz, 1H, H-6), 7.628 (d, J = 15.6 Hz, 1H, H-α), 7.533 (t, 1H, H-5), 7.150 (t, 1H, H-5′), 7.084 (d, J = 8.4 Hz, 1H, H-4), 6.977 (t, 1H, H-4′), 3.989 (s, 3H, OCH_3-2), 3.942 (s, 3H, OCH_3-3). ESI-MS m/z: 281.9 $(M - 1)^-$; calcd for $C_{17}H_{17}NO_3$, 283.32.

*(E)-2,4-Dichloro-4′-methoxychalcone (**20**).* White powder, 88.3% yield, mp 130.0−132.6 °C. ^{1}H NMR ($CDCl_3$), δ: 8.014 (d, J = 8.4 Hz, 2H, H-2′, H-6′), 7.772 (d, J = 15.6 Hz, 1H, H-β), 7.537 (d, J = 9 Hz, 2H, H-2, H-6), 7.342 (d, J = 15.6 Hz, 1H, H-α), 6.960 (d, J = 9 Hz, 2H, H-3, H-5), 6.686 (d, J = 8.4 Hz, 2H, H-3′, H-5′), 3.052 (s, 6H, $N(CH_3)_2$-4′). ESI-MS m/z: 307.5 $(M + 1)^+$, 308.5 $(M + 1)^+$; calcd for $C_{16}H_{12}Cl_2O_2$, 307.17.

*(E)-4-Dimethylamino-4′-methoxychalcone (**21**).* Orange yellow powder, 87.9% yield, mp 115.0−18.0 °C. ^{1}H NMR ($CDCl_3$), δ: 8.014 (d, J = 8.4 Hz, 2H, H-2′, H-6′), 7.772 (d, J = 15.6 Hz, 1H, H-β), 7.537 (d, J = 9 Hz, 2H, H-2, H-6), 7.342 (d, J = 15.6 Hz, 1H, H-α), 6.960 (d, J = 9 Hz, 2H, H-3, H-5), 6.686 (d, J = 8.4 Hz, 2H, H-3′, H-5′), 3.052 (s, 6H, $N(CH_3)_2$-4′). ESI-MS m/z: 282.9 $(M + 1)^+$; calcd for $C_{18}H_{19}NO_2$, 281.35.

*(E)-2-Chloro-4′-methoxychalcone (**23**).* White powder, 96.0% yield, mp 87.8−89.3 °C. ^{1}H NMR ($CDCl_3$), δ: 8.159 (d, J = 16.2 Hz, 1H, H-β), 8.038 (d, J = 9 Hz, 2H, H-2′, H-6′), 7.742 (d, J = 6.6 Hz, 1H, H-3), 7.495 (d, J = 15.6 Hz, 1H, H-α), 7.442 (d, J = 9 Hz, 1H, H-6), 7.326 (t, 1H, H-4), 7.314 (t, 1H, H-5), 6.989 (d, J = 8.4 Hz, 2H, H-3′, H-5′), 3.896 (s, 3H, OCH_3-4′). ESI-MS m/z: 274.2 $(M + 1)^+$; calcd for $C_{16}H_{13}ClO_2$, 272.73.

*(E)-2-Fluoro-4′-methoxychalcone (**25**).* White powder, 91.5% yield, mp 86.3−87.8 °C. ^{1}H NMR ($CDCl_3$), δ: 8.045 (d, J = 7.8 Hz, 2H, H-2′, H-6′), 7.885 (d, J = 15.6 Hz, 1H, H-β), 7.659 (d, J = 16.8 Hz, 1H, H-α), 7.634 (d, J = 7.8 Hz, 1H, H-6), 7.372 (m, 1H, H-4), 7.194 (t, 1H, H-5), 7.131 (d, J = 8.4 Hz, 1H, H-3), 6.988 (d, J = 7.8 Hz, 2H, H-3′, H-5′), 3.894 (s, 3H, OCH_3-4′). ESI-MS m/z: 278.9 (M + 23)$^+$; calcd for $C_{16}H_{13}FO_2$, 256.27

*(E)-4-Hydroxy-4′-methoxychalcone (**27**).* Light yellow powder crystal, 12.6% yield, mp 170.4−171.0 °C. ^{1}H NMR ($CDCl_3$), δ: 10.048 (s, 1H, OH-4), 8.122 (d, J = 8.4 Hz, 2H, H-2′, H-6′), 7.721 (d, J = 8.4 Hz, 2H, H-2, H-6), 7.720 (d, J = 15.6 Hz, 1H, H-β), 7.641 (d, J = 15.6 Hz, 1H, H-α), 7.070 (d, J = 9.0 Hz, 2H, H-3, H-5), 6.834

(d, J = 8.4 Hz, 2H, H-3′, H-5′), 3.860 (s, 3H, OCH_3-4′). ESI-MS m/z: 253.0 $(M - 1)^-$; calcd for $C_{16}H_{14}O_3$, 254.28.

*(E)-2,4,4′,6-Tetramethoxychalcone (**28**).* Yellow powder crystal, 45.3% yield, mp 142.5−144.6 °C. ^{1}H NMR ($CDCl_3$), δ: 8.232 (d, J = 15.6 Hz, 1H, H-β), 8.024 (d, J = 7.8 Hz, 2H, H-2′, H-6′), 7.885 (d, J = 9.6 Hz, 1H, H-α), 6.961 (d, J = 8.4 Hz, 2H, H-3′, H-5′), 6.141 (s, 2H, H-3, H-5), 3.905 (s, 6H, OCH_3-2, OCH_3-6), 3.876 (s, 3H, OCH_3-4′), 3.856 (s, 3H, OCH_3-4). ESI-MS m/z: 329.0 $(M + 1)^+$; calcd for $C_{19}H_{20}O_5$, 328.36.

*(E)-2,3-Dimethoxy-4′-methoxychalcone (**30**).* White powder crystal, 82.6% yield, mp 99.0−99.5 °C. ^{1}H NMR ($CDCl_3$), δ: 8.077 (d, J = 15.6 Hz, 1H, H-β), 8.040 (d, J = 8.4 Hz, 2H, H-2′, H-6′), 7.612 (d, J = 16.2 Hz,1H, H-α), 7.276 (d, J = 7.2 Hz, 1H, H-6), 7.094 (t, 1H, H-5), 6.982 (d, J = 8.4 Hz 2H, H-3′, H-5′), 6.964 (d,J = 7.2 Hz, 1H, H-4), 3.894 (s, 3H, OCH_3-4′), 3.891 (s, 3H, OCH_3-2), 3.886 (s, 3H, OCH_3-3). ESI-MS m/z: 299.2 $(M + 1)^+$; calcd for $C_{18}H_{18}O_4$, 298.33.

*(E)-2-Trifluoromethyl-4′-aminochalcone (**31**).* Light yellow powder, 70.8% yield, mp 50.6−50.8 °C. ^{1}H NMR ($CDCl_3$), δ: 8.105 (d, J = 15.6 Hz, 1H, H-β), 8.024 (d, J = 8.4 Hz, 2H, H-2′, H-6′), 7.817 (d, J = 7.8 Hz, 1H, H-3), 7.722 (d, J = 7.8 Hz, 1H, H-6), 7.597 (t, 1H, H-5), 7.498 (t, 1H, H-4), 7.422 (d, J = 15.6 Hz, 1H, H-α), 6.984 (d, J = 9 Hz, 2H, H-3′, H-5′), 3.891 (s, 3H, OCH_3-4′). ESI-MS m/z: 307.5 $(M + 1)^+$; calcd for $C_{17}H_{13}F_3O_2$, 306.28.

*(E)-2-Bromo-4′-methoxychalcone (**32**).* White powder, 99.0% yield, mp 42.9−43.8 °C. ^{1}H NMR ($CDCl_3$), δ: 8.109 (d, J = 15.6 Hz, 1H, H-β), 8.039 (d, J = 9.0 Hz, 2H, H-2′, H-6′), 7.729 (d, J = 7.8 Hz, 1H, H-6), 7.639 (d, J = 7.8 Hz, 1H, H-3), 7.437 (d, J = 15.6 Hz, 1H, H-α), 7.361 (t, 1H, H-5), 7.246 (t, 1H, H-4), 6.991 (d, J = 9 Hz, 2H, H-3′, H-5′), 3.898 (s, 3H, OCH_3-4′). ESI-MS m/z: 319.7 $(M + 1)^+$; calcd for $C_{16}H_{13}BrO_2$, 317.18.

*(E)-3,4-Dichloro-4′-methoxychalcone (**33**).* Light yellow powder, 68.1% yield, mp 126.0−127.4 °C. ^{1}H NMR ($CDCl_3$), δ: 8.035 (dd, J = 1.8 Hz, 7.2 Hz, 2H, H-2′, H-6′), 7.721 (d, J = 1.8 Hz, 1H, H-2), 7.678 (d, J = 15.6 Hz, 1H, H-β), 7.519 (d, J = 15.6 Hz, 1H, H-α), 7.486 (d, J = 7.8 Hz, 1H, H-5), 7.448 (dd, J = 1.8, 8.4 Hz, 1H, H-6), 6.992 (dd, J = 1.8, 7.2 Hz, 2H, H-3′, H-5′), 3.899 (s, 3H, OCH_3-4′). ESI-MS m/z: 307.3/309.3 $(M + 1)^+$; calcd for $C_{16}H_{12}Cl_2O_2$, 307.17.

*(E)-3,4-Dichloro-4′-methoxychalcone (**34**).* White powder, 83.4% yield, mp 132.5−134.7 °C. ^{1}H NMR ($CDCl_3$), δ: 8.032 (d, J = 8.4 Hz, 2H, H-2′, H-6′), 7.694 (d, J = 15.6 Hz, 1H, H-β), 7.468 (d, J = 8.4 Hz, 1H, H-6), 7.456 (d, 1H, H-α), 7.354 (brs, 1H, H-2), 7.183−7.227 (m, 1H, H-5), 6.991 (d, J = 8.4 Hz, 2H, H-3′, H-5′), 3.899 (s, 3H, OCH_3-4). ESI-MS m/z: 275.9 $(M + 1)^+$; calcd for $C_{16}H_{12}F_2O_2$, 274.26.

*(E)-2,4-Dichloro-2′-hydroxychalcone (**35**).* Light yellow powder, 39.8% yield, mp 162.2−164.4 °C. ^{1}H NMR ($CDCl_3$), δ: 12.002 (s, 1H, OH-2′), 8.224 (d, J = 15 Hz, 1H, H-β), 7.889 (d, J = 7.8 Hz, 1H, H-6′), 7.703 (d, J = 8.4 Hz, 1H, H-6), 7.624 (d, J = 15.6 Hz, 1H, H- α), 7.521 (t, 3H, H-4′), 7.493 (s, 1H, H-3), 7.330 (d, J = 6 Hz, 1H, H-5), 7.037 (t, 1H, H-3′), 6.952 (t, 1H, H-5′). ESI-MS m/z: 291.2 $(M - 1)^-$; calcd for $C_{15}H_{10}Cl_2O_2$, 293.14.

*(E)-2,4,6-Trimethoxy-2′-hydroxychalcone (**37**).* Yellow powder, 8.3% yield, mp 128.3−130.2 °C. ^{1}H NMR ($CDCl_3$), δ: 13.272 (s, 1H, OH-2′), 8.391 (d, J = 15.6 Hz, 1H, H-β), 8.022 (d, J = 15.6 Hz, 1H, H-α), 7.905 (dd, J = 8.1 Hz, 1H, H-6′), 7.436−7.464 (m, 1H, H-4′), 6.998(dd, J = 8.7 Hz, 1H, H- 3′), 6.899−6.926(m, 1H, H-5′), 6.148(s, 2H, H-3, H-5), 3.937 (s, 6H, OCH_3-2, OCH_3-6), 3.872 (s, 3H, OCH_3-4). ESI-MS m/z: 315.4 $(M + 1)^+$; calcd for $C_{18}H_{18}O_5$, 314.33.

*(E)-2,4-Dimethoxy-2′-hydroxychalcone (**38**).* Yellow powder, 54.3% yield, mp 88.3−89.6 °C. ^{1}H NMR ($CDCl_3$), δ: 8.171 (d, J = 15.6 Hz, 1H, H-β), 7.917 (d, J = 8.4 Hz, 1H, H-6′), 7.702 (d, J = 15.6 Hz, 1H, H-α), 7.590 (d, J = 9.0 Hz, 1H, H-6), 7.482 (m, 1H, H-4′), 7.013 (d, J = 8.4 Hz, 1H, H-3′), 6.927 (t, 1H, H-5′), 6.552 (d, J = 9.0 Hz, 1H, H-5), 6.495 (s, 1H, H-3), 3.917 (s, 3H, OCH_3-2), 3.873 (s, 3H, OCH_3-4). ESI-MS m/z: 285.5 $(M + 1)^+$; calcd for $C_{17}H_{16}O_4$, 284.31.

*(E)-2,4-Dimethoxy-3′,4′-difluorochalcone (**39**).* Yellow powder, 83.2% yield, mp 128.8−129.9 °C. ^{1}H NMR ($CDCl_3$), δ: 8.054 (d, J = 15.6 Hz, 1H, H-β), 7.827−7.862 (m, 1H, H-5′), 7.775−7.797 (m, 1H, H-2′), 7.562 (d, J = 8.4 Hz, 1H, H-6), 7.466 (d, J = 15.6 Hz, 1H, H-α), 7.244−7.287 (m, 1H, H-6′), 6.544 (dd, J = 2.4 Hz, 8.4 Hz, 1H, H-5), 6.483 (d, J = 1.8 Hz, 1H, H-3), 3.913 (s, 3H, OCH_3-2), 3.865 (s, 3H, OCH_3-4). ESI-MS m/z: 305.3 $(M + 1)^+$; calcd for $C_{17}H_{14}F_2O_3$, 304.29.

*(E)-2,3′,4,4′,5′-Pentamethoxychalcone (**41**).* Yellow powder, 90.0% yield, mp 125.7−127.7 °C. ^{1}H NMR ($CDCl_3$), δ: 8.047 (d, J = 15.6 Hz, 1H, H-β), 7.578 (d, J = 8.4 Hz, 1H, H-6), 7.475 (d, J = 16.2 Hz, 1H, H-α), 7.263 (s, 2H, H-2′, H-6′), 6.549 (dd, J = 1.8 Hz, 8.4 Hz, 1H, H-5), 6.487 (d, J = 2.4 Hz, 1H, H-3), 3.947 (s, 6H, OCH_3-3′,OCH_3-5′), 3.933 (s, 3H, OCH_3-2), 3.905 (s, 3H, OCH_3-4′), 3.865 (s, 3H, OCH_3-4). ESI-MS m/z: 359.0 $(M + 1)^+$; calcd for $C_{20}H_{22}O_6$, 358.39.

*(E)-2,4-Dichloro-3′,4′-dimethoxychalcone (**42**).* White powder, 87.0% yield, mp 132.2−135.1 °C. ^{1}H NMR ($CDCl_3$), δ: 8.079 (d, J = 15.6 Hz, 1H, H-β), 7.679 (d, J = 8.4 Hz, 1H, H-6′), 7.660 (d, J = 8.4 Hz, 1H, H-6), 7.613 (d, J = 0.6 Hz, 1H, H-3), 7.479 (d, J = 15.0 Hz, 1H, H-α), 7.471 (s, 1H, H-2′), 7.302 (dd, J = 1.2 Hz, 8.4 Hz, 1H, H-5) 6.932 (d, J = 8.4 Hz, 1H, H-5′), 3.943 (s, 6H, OCH_3-3′, OCH_3-4′). ESI-MS m/z: 337.1, 339.1 $(M + 1)^+$; calcd for $C_{17}H_{23}Cl_2O$, 337.2.

*(E)-4-Dimethylamino-3′,4′-dimethoxychalcone (**44**).* Orange yellow powder, 71.8% yield, mp 109.8−113.0 °C. ^{1}H NMR ($CDCl_3$), δ: 7.793 (d, J = 15.6 Hz, 1H, H-β), 7.672 (dd, J = 1.8 Hz, 8.4 Hz, 1H, H-6′), 7.623 (d, J = 1.8 Hz, 1H, H-2′), 7.561 (d, J = 9.0 Hz, 2H, H-2, H-6), 7.369 (d, J = 15.6 Hz, 1H, H-α), 6.924 (d, J = 8.4 Hz, 1H, H-5′), 6.733 (d, J = 7.2 Hz, 2H, H-3, H-5), 3.972 (s, 3H, OCH_3-3′), 3.962 (s, 3H, OCH_3-4′), 3.047 (s, 3H, $N(CH_3)_2$-4). ESI-MS m/z: 312.8 $(M + 1)^+$; calcd for $C_{19}H_{21}O_3$, 311.37.

*(E)-4-Methoxy-3′,4′-dimethoxychalcone (**46**).* White powder, 81.1% yield, mp 83.3−85.2 °C. ^{1}H NMR ($CDCl_3$), δ: 7.778 (d, J = 15.6 Hz, 1H, H-β), 7.677 (dd, J = 1.2, 8.4 Hz, 1H, H-6′), 7.623 (d, J = 1.8 Hz, 1H, H-2′), 7.608 (d, J = 8.4 Hz, 2H, H-3, H-6), 7.446 (d, J = 15.0 Hz, 1H, H-α), 6.940 (d, J = 8.4 Hz, 2H, H-3, H-5), 6.929 (d, J = 7.8 Hz, 1H, H-5′), 3.971 (s, 6H, OCH_3-3′, OCH_3-4′), 3.858 (s, 3H, OCH_3-3). ESI-MS m/z: 299.5 $(M + 1)^+$; calcd for $C_{18}H_{18}O_4$, 298.33.

*(E)-2,3′,4,4′-Tetramethoxychalcone (**47**).* Yellow powder, 74.1% yield, mp 111.3−112.6 °C. ^{1}H NMR ($CDCl_3$), δ: 8.040 (d, J = 15.6 Hz, 1H, H-β), 7.666 (dd, J = 1.8 Hz, 8.4 Hz, 1H, H-6′), 7.6235 (d, J = 1.8 Hz, 1H, H-2′), 7.575 (d, J = 8.4 Hz, 1H, H-6), 7.563 (d, J = 15.6 Hz, 1H, H-α), 6.928 (d, J = 8.4 Hz, 1H, H-6), 6.539 (dd, J = 2.4 Hz, 8.4 Hz, 1H, H-5), 6.482 (d, J = 2.4 Hz, 1H, H-3), 3.970 (s, 3H, OCH_3-4′), 3.962 (s, 3H, OCH_3-3′), 3.905 (s, 3H, OCH_3-2), 3.858 (s, 3H, OCH_3-4). ESI-MS m/z: 329.1 $(M + 1)^+$; calcd for $C_{19}H_{20}O_5$, 328.36.

*(E)-2-Methoxy-3′,5′-difluorochalcone (**54**).* Light yellow powder, 74.1% yield, mp 94.5−96.7 °C. ^{1}H NMR ($CDCl_3$), δ: 8.163 (d, J = 16.2 Hz, 1H, H-β), 7.655 (dd, J = 1.8 Hz, 7.8 Hz, 2H, H-2′, H-6′), 7.543 (dd, J = 1.8, 7.8 Hz, 1H, H-6), 7.544 (d, J = 16.2 Hz, 1H, H-α), 7.439 (dt, J = 1.8, 8.4 Hz, 1H, H-4′), 7.048−7.066 (m, 1H, H-4), 7.034−7.048 (m, 1H, H-5), 6.990 (d, J = 8.4 Hz, 1H, H-3), 3.964 (s, 3H, OCH_3-2). ESI-MS m/z: 274.5 $(M + 1)^+$; calcd for $C_{16}H_{12}F_2O_2$, 274.26.

4.2. Animals. Male ICR mice and C57BL/6 (B6) mice weighing 18−22 g were obtained from the Animal Center of Wenzhou Medical College (Wenzhou, China). Animals were housed at a constant room temperature with a 12/12 h light−dark cycle and fed with a standard rodent diet and water. The animals were acclimatized to the laboratory for at least 7 days before used in experiments. Protocols involving the use of animals were approved by the Wenzhou Medical College Animal Policy and Welfare Committee (approval documents: 2009/APWC/0031).

4.3. Reagents and Cells. Chemical reagents and lipopolysaccharide (LPS) were purchased from Sigma (St. Louis, MO). Saline was prepared as 0.9% NaCl solution. Mouse RAW 264.7 macrophages were obtained from the American Type Culture Collection (ATCC, U.S.). RAW 264.7 macrophages were incubated in DMEM medium (Gibco, Eggenstein, Germany) supplemented with 10% FBS (Hyclone, Logan, UT), 100 U/mL penicillin, and 100 mg/mL streptomycin at 37 °C with 5% CO_2. For peritoneal macrophage preparation, ICR mice were stimulated by intraperitoneal (ip) injection of 3 mL of thioglycollate solution (0.3 g of beef extract, 1 g of tryptone, 0.5 g of sodium chloride, and 6 g of soluble starch were

dissolved and boiled in 100 mL of water; before use, the solution was filtrated with 0.22 μm filter) per mouse and kept in pathogen-free conditions for 3 days before peritoneal macrophage isolation. Total peritoneal macrophages were harvested by washing the peritoneal cavity with PBS containing 30 mM of EDTA (8 mL per mouse) and centrifuged. Then the pellet was resuspended in RPMI-1640 medium (Gibco, Eggenstein, Germany) with 10% FBS (Hyclone, Logan, UT), 100 U/mL penicillin, and 100 mg/mL streptomycin. Nonadherent cells were removed by washing with medium at 3 h after seeding. Experiments were undertaken after the cells adhered firmly to the culture plates. Before use, peritoneal macrophages were cultured in RPMI-1640 medium on 60 mm plates (1.2×10^6 cells in 3 mL of medium per plate) and maintained at 37 °C in a 5% CO_2-humidified air.

4.4. Determination of TNF-α and IL-6. After treatment of cells with indicated compounds and LPS, the TNF-α and IL-6 levels in medium were determined with an ELISA kit (eBioScience, San Diego, CA) according to the manufacturer's instructions. The total amount of the inflammatory factor in the medium was normalized to the total protein quantity of the viable cell pellets.

4.5. Real-Time Quantitative PCR. Cells were homogenized in TRIZOL kit (Invitrogen, Carlsbad, CA) for extraction of RNA according to each manufacturer's protocol. Both reverse transcription and quantitative PCR were carried out using a two-step M-MLV Platinum SYBR Green qPCR SuperMix-UDG kit (Invitrogen, Carlsbad, CA). Eppendorf Mastercycler ep realplex detection system (Eppendorf, Hamburg, Germany) was used for q-PCR analysis. The primers of genes including TNF-α, IL-6, IL-12, IL-1β, COX-2, and β-actin were synthesized by Invitrogen. The primer sequences of mouse genes used are shown as follows:

TNF-α sense primer, 5′-TGGAACTGGCAGAAGAGG-3′;
TNF-α antisense primer, 5′-AGACAGAAGAGCGTGGTG-3′;
IL-6 sense primer, 5′-GAGGATACCACTCCCAACAGACC-3′;
IL-6 antisense primer, 5′-AAGTGCATCATCGTTGTTCATACA-3′;
COX-2 sense primer, 5′-TGGTGCCTGGTCTGATGATG-3′;
COX-2 antisense primer, 5′-GTGGTAACCGCTCAGGTGTTG-3′;
IL-12 sense primer, 5′-GGAAGCACGGCAGCAGAATA-3′;
IL-12 antisense primer, 5′-AACTTGAGGGAGAAGTAGGAATGG-3′;
IL-1β sense primer, 5′-ACTCCTTAGTCCTCGGCCA-3′;
IL-1β antisense primer, 5′-CCATCAGAGGCAAGGAGGAA-3′;
β-actin sense primer, 5′-TGGAATCCTGTGGCATCCATGAAAC-3′;
β-actin antisense primer, 5′-TAAAACGCAGCTCAGTAACAGTCCG-3′.

The amount of each gene was determined and normalized by the amount of β-actin.

4.6. Western Blot Analysis. The treated cells were collected and lysated. Then an amount of 40 μg of the whole cell lysates was separated by 10% sodium dodecyl sulfate−polyacrylamide gel electrophoresis and electrotransferred to a nitrocellulose membrane. Each membrane was preincubated for 1 h at room temperature in Tris-buffered saline, pH 7.6, containing 0.05% Tween 20 and 5% nonfat milk. The nitrocellulose membrane was incubated with specific antibodies against p-JNK, JNK, IκB, p-p38, p38, p-ERK, ERK, or actin (Santa Cruz Biotech Co. Ltd., CA). Immunoreactive bands were then detected by incubating with secondary antibody conjugated with horseradish peroxidase and visualized using enhanced chemiluminescence reagents (Bio-Rad, Hercules, CA).

4.7. Assay of Cellular NF-κB p-65 Translocation. The cells were immunofluorescence-labeled according to the manufacturer's instructions using a cellular NF-κB p-65 translocation kit (Beyotime Biotech, Nantong, China). P65 protein and nuclei fluoresce red and blue and can be simultaneously viewed by fluorescence microscope (Nikon, Tokyo, Japan) at an excitation wavelength of 350 nm for DAPI and 540 nm for Cy3. To create a two-color image, the red and blue images were overlaid, producing purple fluorescence in areas of colocalization.

4.8. LPS-Induced Inflammatory Mortality in B6 Mice. Compounds were first dissolved with macrogol 15 hydroxystearate (a nonionic solubilizer for injection from BASF) with or without medium chain triglycerides (MCT, from BASF) in a water bath at 37 °C. The concentration of compounds was 2 mg/mL. The concentration of solubilizer was 5−10%, and that for MCT was 0.5−2% in final solution. For the vehicle, the mixture of solubilizer and MCT was prepared at 10% and 2%, respectively. Male B6 mice weighing 18−22 g were pretreated with compounds in a water solution (200 μL, 15 mg/kg) by iv injection 15 min before the iv injection of LPS (20 mg/kg). Control animals received a similar volume (200 μL) of vehicle. Body weight change and mortality were recorded for 7 days.

4.9. Statistical Analysis. The results are presented as the mean ± SD. The Student's t test was employed to analyze the differences between sets of data. Statistics were performed using GraphPad Pro (GraphPad, San Diego, CA). P values less than 0.05 ($p < 0.05$) were considered indicative of significance. All experiments were repeated at least three times.

■ ASSOCIATED CONTENT

Ⓢ Supporting Information

Details of quantitative structure−activity relationship (QSAR) study of synthetic chalcones. This material is available free of charge via the Internet at http://pubs.acs.org.

■ AUTHOR INFORMATION

Corresponding Author

*Phone: (+86) 577-86699524. Fax: (+86) 577-86699527. E-mail: wzmcliangguang@163.com.

Author Contributions

§These authors contribute equally to this work.

Notes

The authors declare no competing financial interest.

■ ACKNOWLEDGMENTS

Financial support was provided by the National Natural Science Funding of China (Grants 20802054, 30872308, 81072683), High-Level Innovative Talent Funding of Zhejiang Department of Health (G.L.), Project of Wenzhou Sci-Tech Bureau (Grants Y20090009 and Y20100006), Zhejiang Natural Science Funding (Grants Y2090358, Y2090680, and Y20101108), Wenzhou City Natural Science Funding (Grant Y20100078), and China Postdoctoral Science Foundation (Grants 20090461121 and 201003591).

■ ABBREVIATIONS USED

TNF, tumor necrosis factor; IL, interleukin; LPS, lipopolysaccharide; iNOS, inducible NO synthetase; COX-2, cycloxygenase 2; NF-κB, nuclear factor κB; IκB, nuclear factor κB light polypeptide gene enhancer inhibitor; MAPK, mitogen-activated protein kinase; ERK, extracellular signal-regulated kinase; JNK, c-Jun-NH_2-terminal kinase

■ REFERENCES

(1) Atreya, R.; Mudter, J.; Finotto, S.; Müllberg, J.; Jostock, T.; Wirtz, S.; Schütz, M.; Bartsch, B.; Holtmann, M.; Becker, C.; et al. Blockade of interleukin 6 trans signaling suppresses T-cell resistance against

apoptosis in chronic intestinal inflammation: evidence in Crohn disease and experimental colitis in vivo. *Nat. Med.* **2000**, *6*, 583−588.
(2) Kalogeropoulos, A.; Georgiopoulou, V.; Psaty, B.; Rodondi, N.; Smith, A.; Harrison, D.; Liu, Y.; Hoffmann, U.; Bauer, D.; Newman, A. Inflammatory markers and incident heart failure risk in older adults the health ABC (health, aging, and body composition) study. *J. Am. Coll. Cardiol.* **2010**, *55*, 2129−2137.
(3) Ait-Oufella, H.; Taleb, S.; Mallat, Z.; Tedgui, A. Recent advances on the role of cytokines in atherosclerosis. *Arterioscler., Thromb., Vasc. Biol.* **2011**, *31*, 969−979.
(4) McInnes, I.; Schett, G. Cytokines in the pathogenesis of rheumatoid arthritis. *Nat. Rev. Immunol.* **2007**, *7*, 429−442.
(5) Grivennikov, S. I.; Karin, M. Inflammatory cytokines in cancer: tumour necrosis factor and interleukin 6 take the stage. *Ann. Rheum. Dis.* **2011**, *70* (Suppl. 1), i104−i108.
(6) Qiu, Y.; Yanase, T.; Hu, H.; Tanaka, T.; Nishi, Y.; Liu, M.; Sueishi, K.; Sawamura, T.; Nawata, H. Dihydrotestosterone suppresses foam cell formation and attenuates atherosclerosis development. *Endocrinology* **2010**, *151*, 3307−3316.
(7) Mazor, R.; Itzhaki, O.; Sela, S.; Yagil, Y.; Cohen-Mazor, M.; Yagil, C.; Kristal, B. Tumor necrosis factor-alpha: a possible priming agent for the polymorphonuclear leukocyte-reduced nicotinamide-adenine dinucleotide phosphate oxidase in hypertension. *Hypertension* **2010**, *55*, 353−362.
(8) Duffield, J. S. Macrophages and immunologic inflammation of the kidney. *Semin. Nephrol.* **2010**, *30*, 234−254.
(9) Moore, K. J.; Tabas, I. Macrophages in the pathogenesis of atherosclerosis. *Cell* **2011**, *145*, 341−355.
(10) Yadav, V. R.; Prasad, S.; Sung, B.; Aggarwal, B. B. The role of chalcones in suppression of NF-kappaB-mediated inflammation and cancer. *Int. Immunopharmacol.* **2011**, *11*, 295−309.
(11) Bashir, R.; Ovais, S.; Yaseen, S.; Hamid, H.; Alam, M. S.; Samim, M.; Singh, S.; Javed, K. Synthesis of some new 1,3,5-trisubstituted pyrazolines bearing benzene sulfonamide as anticancer and anti-inflammatory agents. *Bioorg. Med. Chem. Lett.* **2011**, *21*, 4301−4305.
(12) Kumar, V.; Kumar, S.; Hassan, M.; Wu, H.; Thimmulappa, R. K.; Kumar, A.; Sharma, S. K.; Parmar, V. S.; Biswal, S.; Malhotra, S. V. Novel chalcone derivatives as potent Nrf2 activators in mice and human lung epithelial cells. *J. Med. Chem.* **2011**, *54*, 4147−4159.
(13) Srinivasan, B.; Johnson, T. E.; Lad, R.; Xing, C. Structure−activity relationship studies of chalcone leading to 3-hydroxy-4,3′,4′,5′-tetramethoxychalcone and its analogues as potent nuclear factor kappaB inhibitors and their anticancer activities. *J. Med. Chem.* **2009**, *52*, 7228−7235.
(14) Bharate, S. B.; Mahajan, T. R.; Gole, Y. R.; Nambiar, M.; Matan, T. T.; Kulkarni-Almeida, A.; Balachandran, S.; Junjappa, H.; Balakrishnan, A.; Vishwakarma, R. A. Synthesis and evaluation of pyrazolo[3,4-*b*]pyridines and its structural analogues as TNF-alpha and IL-6 inhibitors. *Bioorg. Med. Chem.* **2008**, *16*, 7167−7176.
(15) Lorenzo, P.; Alvarez, R.; Ortiz, M. A.; Alvarez, S.; Piedrafita, F. J.; de Lera, A. R. Inhibition of IkappaB kinase-beta and anticancer activities of novel chalcone adamantyl arotinoids. *J. Med. Chem.* **2008**, *51*, 5431−5440.
(16) Rao, Y. K.; Fang, S. H.; Tzeng, Y. M. Synthesis and biological evaluation of 3′,4′,5′-trimethoxychalcone analogues as inhibitors of nitric oxide production and tumor cell proliferation. *Bioorg. Med. Chem.* **2009**, *17*, 7909−7914.
(17) Meng, C. Q.; Ni, L.; Worsencroft, K. J.; Ye, Z.; Weingarten, M. D.; Simpson, J. E.; Skudlarek, J. W.; Marino, E. M.; Suen, K. L.; Kunsch, C.; Souder, A.; Howard, R. B.; Sundell, C. L.; Wasserman, M. A.; Sikorski, J. A. Carboxylated, heteroaryl-substituted chalcones as inhibitors of vascular cell adhesion molecule-1 expression for use in chronic inflammatory diseases. *J. Med. Chem.* **2007**, *50*, 1304−1315.
(18) Bandgar, B. P.; Patil, S. A.; Gacche, R. N.; Korbad, B. L.; Hote, B. S.; Kinkar, S. N.; Jalde, S. S. Synthesis and biological evaluation of nitrogen-containing chalcones as possible anti-inflammatory and antioxidant agents. *Bioorg. Med. Chem. Lett.* **2010**, *20*, 730−733.
(19) Bandgar, B. P.; Patil, S. A.; Korbad, B. L.; Nile, S. H.; Khobragade, C. N. Synthesis and biological evaluation of beta-chloro vinyl chalcones as inhibitors of TNF-alpha and IL-6 with antimicrobial activity. *Eur. J. Med. Chem.* **2010**, *45*, 2629−2633.
(20) Consonni, V.; Todeschini, R.; Pavan, M. Structure/response correlations and similarity/diversity analysis by GETAWAY descriptors. 1. Theory of the novel 3D molecular descriptors. *J. Chem. Inf. Comput. Sci.* **2002**, *42*, 682−692.
(21) Gasteiger, J.; Sadowski, J.; Schuur, J.; Selzer, P.; Steinhauer, L.; Steinhauer, V. Chemical information in 3D space. *J. Chem. Inf. Comput. Sci.* **1996**, *36*, 1030−1037.
(22) Todeschini, R.; Consonni, V. *Handbook of Molecular Descriptors*, 1st ed.; Wiley-VCH: Mannheim, Germany, 2000.
(23) Dinarello, C. A. Interleukin-1 in the pathogenesis and treatment of inflammatory diseases. *Blood* **2011**, *117*, 3720−3732.
(24) White, M.; Mahon, V.; Grealy, R.; Doherty, D. G.; Stordeur, P.; Kelleher, D. K.; McManus, R.; Ryan, T. Post operative infection and sepsis in humans is associated with deficient gene expression of gammac cytokines and their apoptosis mediators. *Crit Care* **2011**, *15*, R158.
(25) Li, C. Y.; Chao, L. K.; Wang, S. C.; Chang, H. Z.; Tsai, M. L.; Fang, S. H.; Liao, P. C.; Ho, C. L.; Chen, S. T.; Cheng, W. C.; Chiang, C. S.; Kuo, Y. H.; Hua, K. F.; Hsu, I. C. Honokiol inhibits LPS-induced maturation and inflammatory response of human monocyte-derived dendritic cells. *J. Cell. Physiol.* **2011**, *226*, 2338−2349.
(26) Hiransai, P.; Ratanachaiyavong, S.; Itharat, A.; Graidist, P.; Ruengrairatanaroj, P.; Purintrapiban, J. Dioscorealide B suppresses LPS-induced nitric oxide production and inflammatory cytokine expression in RAW 264.7 macrophages: the inhibition of NF-kappaB and ERK1/2 activation. *J. Cell. Biochem.* **2010**, *109*, 1057−1063.
(27) Furusawa, J.; Funakoshi-Tago, M.; Tago, K.; Mashino, T.; Inoue, H.; Sonoda, Y.; Kasahara, T. Licochalcone A significantly suppresses LPS signaling pathway through the inhibition of NF-kappaB p65 phosphorylation at serine 276. *Cell. Signalling* **2009**, *21*, 778−785.
(28) Guha, M.; Mackman, N. LPS induction of gene expression in human monocytes. *Cell. Signalling* **2001**, *13*, 85−94.
(29) Lee, Y. J.; Kang, D. G.; Kim, J. S.; Lee, H. S. Effect of *Buddleja officinalis* on high-glucose-induced vascular inflammation in human umbilical vein endothelial cells. *Exp. Biol. Med. (Maywood, NJ, U. S.)* **2008**, *233*, 694−700.
(30) Stan, D.; Calin, M.; Manduteanu, I.; Pirvulescu, M.; Gan, A. M.; Butoi, E. D.; Simion, V.; Simionescu, M. High glucose induces enhanced expression of resistin in human U937 monocyte-like cell line by MAPK- and NF-kB-dependent mechanisms; the modulating effect of insulin. *Cell Tissue Res.* **2010**, *343*, 379−387.
(31) Voilley, N. Acid-sensing ion channels (ASICs): new targets for the analgesic effects of non-steroid anti-inflammatory drugs (NSAIDs). *Curr. Drug Targets: Inflammation Allergy* **2004**, *3*, 71−79.
(32) Choi, J. M.; Yoon, B. S.; Lee, S. K.; Hwang, J. K.; Ryang, R. Antioxidant properties of neohesperidin dihydrochalcone: inhibition of hypochlorous acid-induced DNA strand breakage, protein degradation, and cell death. *Biol. Pharm. Bull.* **2007**, *30*, 324−330.
(33) Nabi, G.; Liu, Z. Q. Radical-scavenging properties of ferrocenyl chalcones. *Bioorg. Med. Chem. Lett.* **2011**, *21*, 944−946.
(34) Barona, I.; Fagundes, D. S.; Gonzalo, S.; Grasa, L.; Arruebo, M. P.; Plaza, M. A.; Murillo, M. D. Role of TLR4 and MAPK in the local effect of LPS on intestinal contractility. *J. Pharm. Pharmacol.* **2011**, *63*, 657−662.
(35) Han, J. M.; Jin, Y. Y.; Kim, H. Y.; Park, K. H.; Lee, W. S.; Jeong, T. S. Lavandulyl flavonoids from *Sophora flavescens* suppress lipopolysaccharide-induced activation of nuclear factor-kappaB and mitogen-activated protein kinases in RAW264.7 cells. *Biol. Pharm. Bull.* **2010**, *33*, 1019−1023.
(36) Shim, J. S.; Kwon, Y. Y.; Han, Y. S.; Hwang, J. K. Inhibitory effect of panduratin A on UV-induced activation of mitogen-activated protein kinases (MAPKs) in dermal fibroblast cells. *Planta Med.* **2008**, *74*, 1446−1450.

(37) Kim, Y. J.; Ko, H.; Park, J. S.; Han, I. H.; Amor, E. C.; Lee, J. W.; Yang, H. O. Dimethyl cardamonin inhibits lipopolysaccharide-induced inflammatory factors through blocking NF-kappaB p65 activation. *Int. Immunopharmacol.* **2010**, *10*, 1127−1134.
(38) Rittirsch, D.; Flierl, M. A.; Day, D. E.; Nadeau, B. A.; McGuire, S. R.; Hoesel, L. M.; Ipaktchi, K.; Zetoune, F. S.; Sarma, J. V.; Leng, L.; Huber-Lang, M. S.; Neff, T. A.; Bucala, R.; Ward, P. A. Acute lung injury induced by lipopolysaccharide is independent of complement activation. *J. Immunol.* **2008**, *180*, 7664−7672.
(39) Soriano, F. G.; Lorigados, C. B.; Pacher, P.; Szabo, C. Effects of a potent peroxynitrite decomposition catalyst in murine models of endotoxemia and sepsis. *Shock* **2011**, *35*, 560−566.
(40) Yozai, K.; Shikata, K.; Sasaki, M.; Tone, A.; Ohga, S.; Usui, H.; Okada, S.; Wada, J.; Nagase, R.; Ogawa, D.; Shikata, Y.; Makino, H. Methotrexate prevents renal injury in experimental diabetic rats via anti-inflammatory actions. *J. Am. Soc. Nephrol.* **2005**, *16*, 3326−3338.
(41) Navarro-Gonzalez, J. F.; Mora-Fernandez, C. The role of inflammatory cytokines in diabetic nephropathy. *J. Am. Soc. Nephrol.* **2008**, *19*, 433−442.